Korean J. Chem. Eng., 38(2), 422-441 (2021)
DOI: 10.1007/s11814-020-0696-x

pISSN: 0256-1115
eISSN: 1975-7220

Modeling of autocatalytic degradation of polymer microparticles with various morphologies based on analytical solutions of reaction-diffusion equations

Young-Sang Cho†

Department of Chemical Engineering and Biotechnology, Korea Polytechnic University,
237 Sangdaehak-ro, Siheung-si, Gyeonggi-do 15073, Korea
(*Received 15 June 2020 • Revised 22 September 2020 • Accepted 14 October 2020*)

Abstract−Analytical solutions of transient concentration of degraded components inside cylindrical and slab-type PLGA particles immersed in infinite medium were derived by solving reaction-diffusion equations of autocatalytic reaction using eigenfunction expansion method. The resulting average concentrations were compared with the modeling results of spherical PLGA particles by Versypt and her colleagues to study the effect of particle morphology on the autocatalytic reaction. Mass transfer resistance inside and outside of the particles was also considered using *Biot* number, and its effects on the concentration inside particles with various morphologies were also studied by solving reaction-diffusion equation. To predict transient concentration in surrounding medium, coupled differential equations were solved for the three shapes of PLGA particles by assuming finite volume of the decomposition system. Mathematical solutions were obtained by Laplace transform, and the results were compared for the PLGA particles with different shapes depending on Thiele modulus and particle volume fraction.

Keywords: Polymer Degradation, Reaction-diffusion Equation, Eigenfunction Expansion, Coupled Differential Equations, Laplace Transform

INTRODUCTION

Over several decades, biodegradable polymers have been investigated for various biomedical applications, especially for tissue engineering, biomedical engineering, or controlled release of drug delivery system [1-3]. Among various kinds of biodegradable polymers, polylactic acid (PLA) or poly(lactic-co-glycolic acid) (PLGA) have been studied intensively because of their excellent bio-compatibility and facile synthesis method as controllable morphologies [4-6]. Though such polymers are often prepared in the form of microspheres from emulsion droplets or nanoparticles, other types of biodegradable polymers are also being investigated by electrospinning for fabrication of cylindrical microparticles considered as almost infinite length [7-10].

The degradation mechanism of biodegradable polymer such as PLGA has been studied in detail [11]. Since degraded product from PLGA acts as another reactant in the reaction, it has been studied as an autocatalytic reaction [12]. Versypt et al. made a meaningful contribution through modeling of PLGA microsphere by solving reaction-diffusion equation, assuming irreversible first-order reaction, which was confirmed experimentally to determine the rate constant from reaction kinetics [13,14]. Since the measurement of the concentration of degradation product inside a PLGA particle is very difficult, it can be predicted through modeling and mathematical solution of reaction-diffusion equation. Additionally, erosion and transport mechanism of molecular flow from particle surface can be understood by the mathematical results after modeling.

As the first modeling of degradation reaction of biodegradable polymer by solving reaction-diffusion equation, Versypt et al. predicted the concentration profile and transient concentration of the degraded product inside a PLGA microsphere [14]. Since this valuable contribution was only made for microspheres, it is necessary to perform computations of the concentration inside other types of particles, such as cylindrical or slab-type particle, and compare the results to study the effect of particle morphology. Because mass transfer resistance in surrounding medium cannot be ignored in a real system, the *Biot* number with finite value can be also considered as boundary condition at the particle surface for more precise calculation of concentration profile. Another important factor of the degradation system can be volume fraction of the particles in finite liquid medium to predict the concentration of degraded component in bulk phase. These additional points can be considered in modeling steps, which are important for mathematical analysis of a biochemical system.

Since various generation or destruction terms can be considered in reaction-diffusion equations, mathematical or numerical descriptions of such equations have been studied intensively for various applications, such as catalytic materials or viral infection systems [15,16]. Because physicochemical insights and understanding of such systems can be provided from the exact analytical solutions of the reaction-diffusion equations, eigenfunction expansion or Laplace transform approaches have been adopted for solving the equations without using numerical tools via computer [17,18]. Thus, derivation of analytical solutions of reaction-diffusion equation for degradation of biodegradable polymers is still important for biochemical engineers.

†To whom correspondence should be addressed.
E-mail: yscho78@kpu.ac.kr, yscho78@gmail.com

In this study, transient concentration as well as concentration distribution of degradation component inside bio-degradable polymeric particles was predicted by solving reaction-diffusion equations in cylindrical or slab-type particle using eigenfunction expansion method. The results were compared with the computation results from spherical particles by Versypt and her colleagues to study the effect of particle shape as well as Thiele modulus. To consider diffusional resistance inside particles to convective resistance in surrounding medium, boundary conditions at the particle surface were revised using *Biot* number, and the results were compared for the three types of the particles. To overcome the restrictions of a isolated particle surrounded in infinite medium, coupled differential equations were modeled to predict concentration in bulk medium as well as concentration inside the particles with fixed volume fraction immersed in finite amount of liquid. The systems of differential equations were solved by Laplace transform, and the results were compared for each particle with varying vales of Thiele modulus and particle volume fraction.

COMPUTATION METHODS

For mathematical modeling, uni-axial diffusion of degraded components has been assumed in all coordinate systems. For instance, diffusional mass transport in polar and azimuthal angle was ignored in spherical coordinate for modeling of degradation of spherical particles. Similarly, diffusion flux in azimuthal angle and height was also ignored in cylindrical coordinate to explain decomposition of biodegradable fibers. In slab-type particles, uniaxial-diffusion along r-direction shown in Fig. 1 was also assumed for modeling and computation.

To compute eigenvalues from transcendental equations, Desmos graphic calculator was used via Internet instead of Newton-Raphson method. Though most graphs and figures in this article were obtained from exact analytical solution of reaction-diffusion equation, numerical solutions were also obtained using MATLAB software for 3D graphics of concentration profile as a function of reaction time.

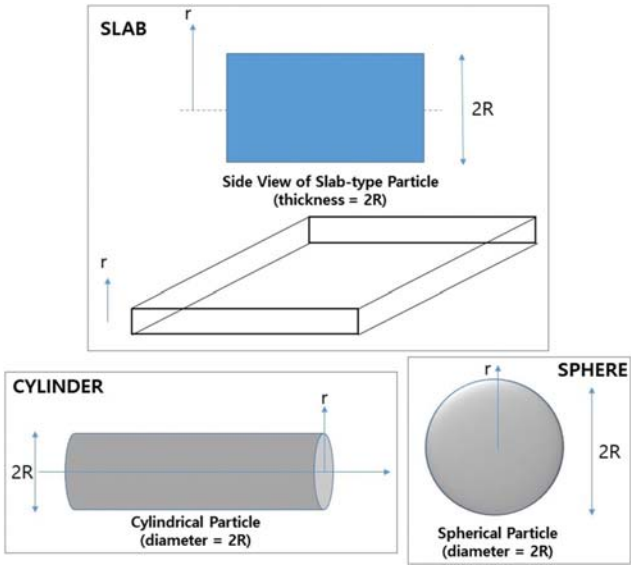

Fig. 1. Schematic figure of biodegradable polymeric particles with slab, cylinder, and spherical morphologies.

RESULTS AND DISCUSSION

1. Transient Concentration Profile Inside Particle with Various Morphologies Immersed in Infinite Medium

Assuming a spherical particle surrounded by infinite medium, transient concentration of product has been already obtained by solving reaction diffusion equation using eigenfunction expansion method, when reaction product is generated by the first-order reaction with rate constant of k [19]. When the initial concentration inside the particle, c_{t0}, and bulk concentration c_{r1} are assumed as constant values, the following reaction-diffusion equation can be derived and solved analytically, when dimensionless reaction time, τ, is defined as $\frac{D}{R^2}t$, where D and R denote diffusion coefficient and radius of particle, respectively.

$$\frac{\partial c}{\partial \tau}=\frac{1}{r^z}\frac{\partial}{\partial r}\left(r^z\frac{\partial c}{\partial r}\right)+\phi^2 c \tag{1}$$

Here, the value of z is 2 for spherical coordinates and ϕ is Thiele modulus, which is defined as $\sqrt{\frac{k}{D}}R$. As reported by Versypt et al., the concentration of product by autocatalytic degradation reaction of PLGA microspheres can be predicted using the following equation as a function of dimensionless reaction time τ and dimensionless distance from the center of the particle, r.

$$c(r,\tau)=\frac{c_{r1}\sin(\phi r)}{r\sin\phi}+2\sum_{n=1}^{\infty}\left(\frac{c_{r1}n\pi}{n^2\pi^2-\phi^2}-\frac{c_{t0}}{n\pi}\right)(-1)^n\exp[(\phi^2-n^2\pi^2)\tau]\frac{\sin(n\pi r)}{r} \tag{2}$$

The above solution has been derived using the boundary conditions such as symmetric boundary condition at the center of the particle and $c(1,\tau)=c_{r1}$ as well as initial condition, $c(r,0)=c_{t0}$ [13]. To avoid computational complexity, the initial concentration, c_{t0}, was assumed as constant value. For convenience, bulk concentration of product, c_{r1} can be also assumed as 0 to obtain the following concentration profile of product for fixed time.

$$\frac{c(r,\tau)}{c_{t0}}=-2\sum_{n=1}^{\infty}\frac{(-1)^n}{n\pi}\exp[(\phi^2-n^2\pi^2)\tau]\frac{\sin(n\pi r)}{r} \tag{3}$$

The concentration at the center of the spherical particle can be obtained by substituting r=0 in the above equation after applying L'Hospital's theorem. By defining average concentration, $\bar{c}(\tau)$, as $\bar{c}(\tau)=\int_0^1 r^2 c(r,\tau)dr$, average concentration inside particle can be obtained as the following equation:

$$\bar{c}(\tau)=-3\frac{c_{r1}}{\phi}\cot\phi+\frac{3c_{r1}}{\phi^2}+3\sum_{n=1}^{\infty}\left(\frac{2c_{t0}}{n\pi}-\frac{2c_{r1}n\pi}{n^2\pi^2-\phi^2}\right)\frac{1}{n\pi}\exp[(\phi^2-n^2\pi^2)\tau] \tag{4}$$

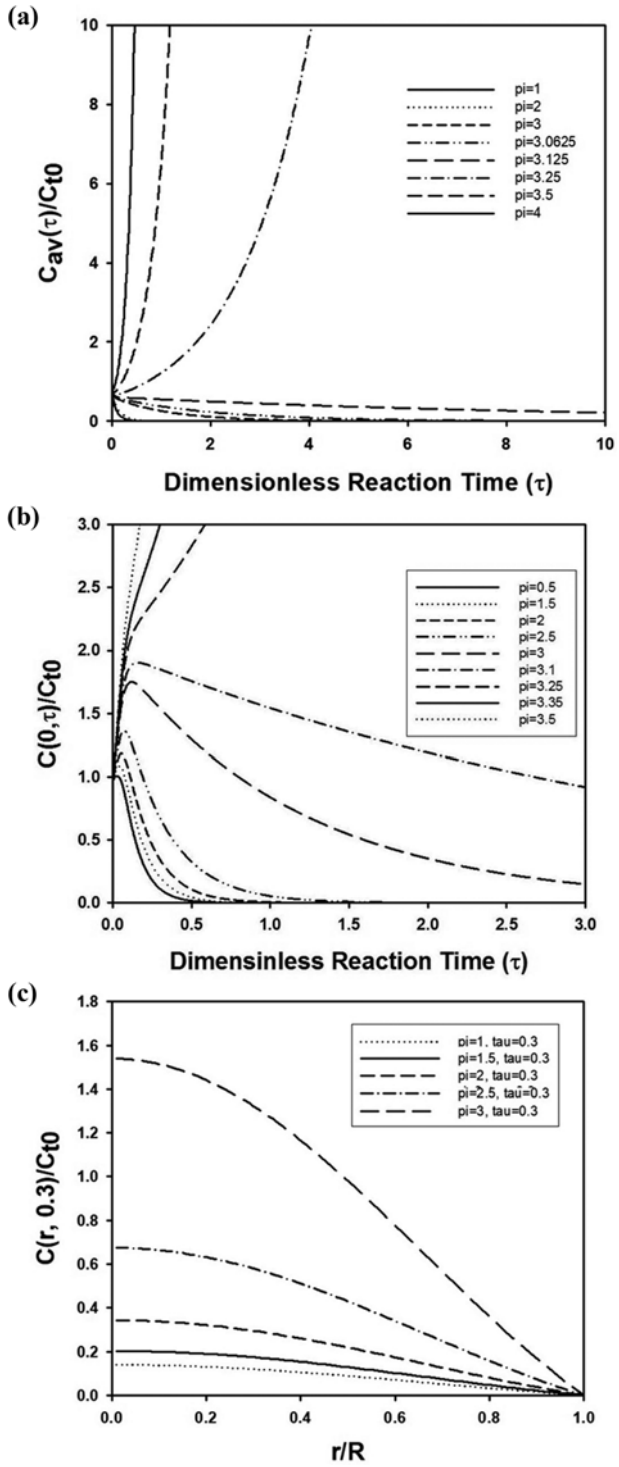

Fig. 2. Change of (a) dimensionless average concentration of degradation product inside spherical PLGA particle and (b) dimensionless concentration of degradation product at the center of the spherical PLGA particle as a function of dimensionless reaction time for various values of Thiele modulus. (c) Concentration profile of degradation product inside spherical PLGA particle as a function of dimensionless radial distance from the center of the particle for τ=0.3 and various values of Thiele modulus. The particle was modeled as immersed body in infinite medium, and the concentration of the product in the medium, C_{r1} was assumed as 0.

Fig. 2(a) contains change of average dimensionless concentration of degradation product inside PLGA microsphere as a function of dimensionless reaction time, when bulk concentration of surrounding medium, c_{r1} is maintained as 0 in Eq. (4). The average concentration decreased when Thiele modulus was smaller than 3.125, whereas it increased rapidly as autocatalytic reaction progressed when Thiele modulus was larger than 3.25. This implies that mass transfer rate of degradation product by diffusion to particle surface is faster than generation rate of the product in the initial stage of the autocatalytic reaction for ϕ is smaller than 4. However, the concentration of the degradation product at the particle center increased consistently when ϕ was larger than 3.2, as displayed in Fig. 2(b). However, the concentration at the particle center decreased as a function of τ after initial rise for short period, since generation rate of the reaction product was not sufficient to maintain high concentration during consistent mass flux outside of the particle for small value of rate constant or ϕ.

For comparison with other geometries, a transient concentration profile of reaction product inside spherical PLGA particles was plotted in Fig. 2(c) for fixed value of reaction time, τ=0.3. Since the boundary condition on the particle surface can be considered as simple mathematical expression like $c(1, \tau)=c_{r1}$, the graph in Fig. 2(c) was plotted by assuming $c_{r1}=0$. Thus, every curve in Fig. 2(c) shows zero concentration at the particle surface regardless of the value of Thiele modulus, ϕ. After uniform initial dimensionless concentration ($c(r, \tau)/c_{t0}=1$), the concentration profile changed to convex shape due to generation of degradation product inside particle and outward mass flux of the product through the particle surface. With increasing value of ϕ, the concentration near central region of the spherical particle increased due to increase of reaction rate.

In addition to spherical particles, degradation of cylindrical PLGA particles immersed in infinite medium can be also modeled to predict the concentration of degradation product inside the cylindrical particles. Since electrospinning can be adopted to fabricate cylindrical PLGA particles with uniform thickness and almost infinite length, cylindrical morphology can be also considered as important as spherical PLGA particles for biodegradable drug carrier [20]. In cylindrical coordinates, the value of z in Eq. (1) can be set as 1 during modeling of reaction-diffusion phenomena, assuming first-order reaction rate. Similar to spherical particles, the following initial and boundary conditions can be considered for analytical solution.

$$\text{Boundary conditions: } \frac{\partial c}{\partial r}=0 \text{ at } r=0 \text{ and } c(1, \tau)=c_{r1} \tag{5}$$

$$\text{Initial condition: } c(r, 0)=c_{t0} \tag{6}$$

Since the second boundary condition is not homogeneous, the solution $c(r, \tau)$ should be divided as $c(r, \tau)=v(r, \tau)+w(r)$, where v and w indicate transient and steady-state solution, respectively, to yield the following differential equations.

$$\frac{\partial v}{\partial \tau}=\frac{1}{r}\frac{\partial}{\partial r}\left(r\frac{\partial v}{\partial r}\right)+\phi^2 v \text{ subject to } \left(\frac{\partial v}{\partial r}\right)_{r=0}=0, v(1, \tau)=0,$$
$$\text{and } v(r, 0)=c(r, 0)-w(r) \tag{7}$$

$$\frac{1}{r}\frac{d}{dr}\left(r\frac{dw}{dr}\right)+\phi^2 w=0 \text{ subject to } \left(\frac{dw}{dr}\right)_{r=0}=0 \text{ and } w(1)=c_{r1} \tag{8}$$

Here, w(r) can be solved as the form of Bessel function of the first kind with order 0 by Frobenius method.

$$w(r)=c_{r1}\frac{J_0(\phi r)}{J_0(\phi)} \tag{9}$$

Eigenfunction expansion method can be applied to solve Eq. (7) by defining operators $\underline{\underline{L}}$ and ξ_n in the following manner.

$$\underline{\underline{L}}=\frac{1}{r}\frac{d}{dr}\left(r\frac{d}{dr}\right)+\phi^2 \text{ and } \underline{\underline{L}}K_n=-\xi_n^2K_n \tag{10}$$

Here, K_n denotes eigenfunction, which can be obtained by solving the following eigenvalue equation.

$$\frac{1}{r}\frac{d}{dr}\left(r\frac{dK_n}{dr}\right)+\phi^2K_n=-\xi_n^2K_n \tag{11}$$

By defining eigenvalue λ_n as $\lambda_n^2=\phi^2+\xi_n^2$, eigenfunction can be solved as Bessel function, $K_n(x)=J_0(\lambda_n x)$. Thus, eigenfunction expansion of $v(r, \tau)$ is possible using time dependent coefficient $a_n(\tau)$ in the following manner.

$$\begin{aligned} v(r,\tau)&=\sum_{n=1}^{\infty}a_n(\tau)J_0(\lambda_n r) \text{ and } v(r,0)\\ &=\sum_{n=1}^{\infty}a_n(0)J_0(\lambda_n r)=c_{t1}-c_{r1}\frac{J_0(\phi r)}{J_0(\phi)}\end{aligned} \tag{12}$$

Since reaction-diffusion equation in cylindrical coordinate can be expressed as $\frac{\partial v}{\partial \tau}=\underline{\underline{L}}v$, $a_n(\tau)$ can be determined by solving an ordinary differential equation, $\frac{da_n}{d\tau}+\xi_n^2a_n=0$. Thus, the coefficient can be expressed as $a_n(\tau)=a_n(0)\exp\{(\phi^2-\lambda_n^2)\tau\}$. Due to orthogonal condition of eigenfunctions, $a_n(0)$ can be determined as the following inner product equation.

$$\begin{aligned} a_n(0)&=\frac{\langle v(r,0), J_0(\lambda_n r)\rangle}{\langle K_n, K_n\rangle}=\frac{\int_0^1 r\left[c_{t1}-c_{r1}\frac{J_0(\phi r)}{J_0(\phi)}\right]J_0(\lambda_n r)dr}{\int_0^1 rJ_0^2(\lambda_n r)dr}\\ &=\frac{\left(\frac{c_{t1}}{\lambda_n}-\frac{c_{r1}}{\phi+\lambda_n}\right)J_1(\lambda_n)}{\frac{1}{2}J_1^2(\lambda_n)}\end{aligned} \tag{13}$$

Thus, the concentration of degradation product inside cylindrical particles, $c(r, \tau)$ can be obtained as the following solution.

$$c(r,\tau)=\frac{c_{r1}J_0(\phi r)}{J_0(\phi)}+2\sum_{n=1}^{\infty}\left(\frac{c_{t1}}{\lambda_n}-\frac{c_{r1}}{\phi+\lambda_n}\right)\exp[(\phi^2-\lambda^2)\tau]\frac{J_0(\lambda_n r)}{J_1(\lambda_n)} \tag{14}$$

Since $J_0(0)=1$ and $J_0(\lambda_n)=0$, transient concentration of the product at the particle center, $c(0, \tau)$ can be easily obtained as the following equation.

$$c(0,\tau)=\frac{c_{r1}}{J_0(\phi)}+2\sum_{n=1}^{\infty}\left(\frac{c_{t1}}{\lambda_n}-\frac{c_{r1}}{\phi+\lambda_n}\right)\exp[(\phi^2-\lambda^2)\tau]\frac{1}{J_1(\lambda_n)} \tag{15}$$

Average concentration inside cylindrical particle can be also found from its definition, $\bar{c}(\tau)=\int_0^2 rc(r,\tau)dr$.

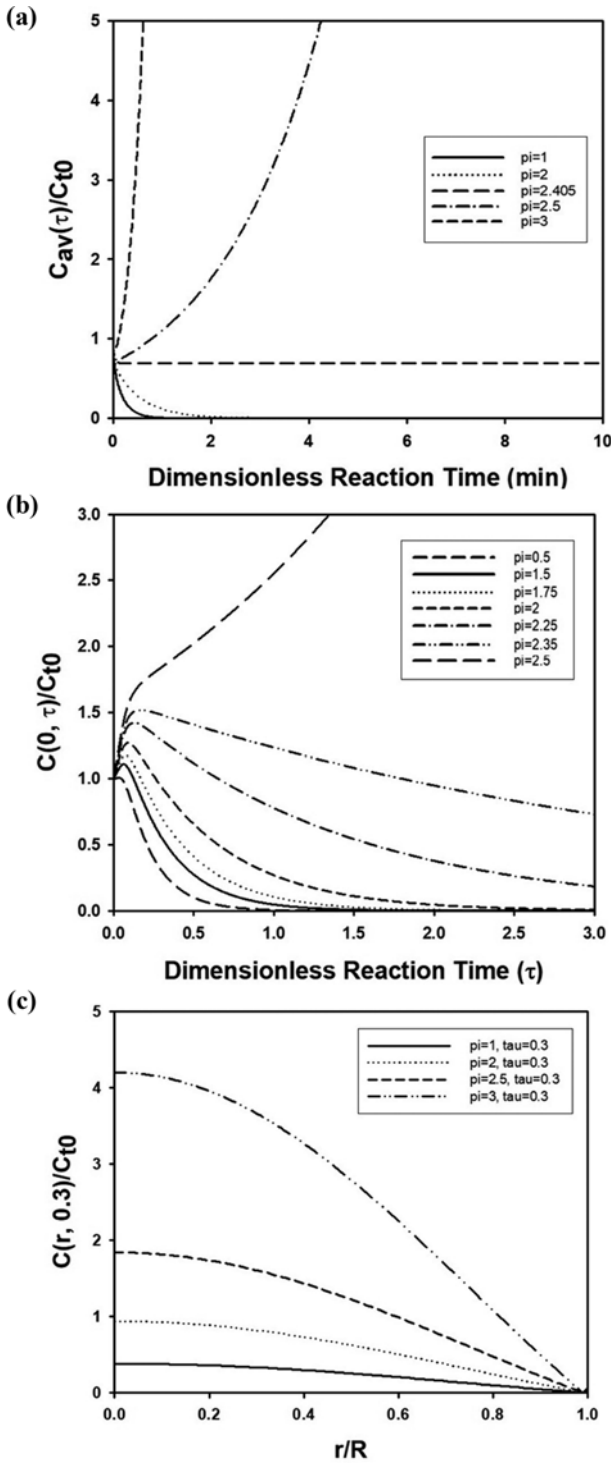

Fig. 3. Change of (a) dimensionless average concentration of degradation product inside cylindrical PLGA particle and (b) dimensionless concentration of degradation product at the center of the cylindrical PLGA particle as a function of dimensionless reaction time for various values of Thiele modulus. (c) Concentration profile of degradation product inside cylindrical PLGA particle as a function of dimensionless radial distance from the center of the particle for τ=0.3 and various values of Thiele modulus. The particle was modeled as immersed body in infinite medium, and the concentration of the product in the medium, C_{r1} was assumed as 0.

$$\bar{c}(\tau)=2\frac{c_{r1}J_1(\phi)}{\phi J_0(\phi)}+4\sum_{n=1}^{\infty}\left(\frac{c_{t1}}{\lambda_n}-\frac{c_{r1}}{\phi+\lambda_n}\right)\exp[(\phi^2-\lambda^2)\tau] \quad (16)$$

Numerical values of eigenvalues, λ_n, can be obtained graphically by solving transcendental equation, $J_0(\lambda_n)=0$, and the digits can be found elsewhere [21].

Fig. 3(a) contains change of average dimensionless concentration of degraded product in cylindrical particles as a function of dimensionless reaction time, when bulk concentration, c_{r1}, is set to 0. When Thiele modulus ϕ is smaller than 2.405, the dimensionless concentration decreases with reaction time, implying that reaction rate is not sufficient to overcome outward flux of the product toward surrounding medium. However, the average concentration increases drastically after slight decrease during initial stage of reaction when ϕ is larger than 2.405, as shown in Fig. 3(a). Thus, the threshold value of the Thiele modulus in cylindrical particles was determined as about 2.405, which is smaller than that in spherical particles. Since the surface area of a sphere is larger than of a cylinder, much higher reaction rate is necessary in spherical particles to compensate outward diffusional flux of degradation product through the particle surface. Unlike average concentration, concentration at r=0 in cylindrical particle increased with increasing reaction time in initial stage of reaction regardless of the value of ϕ, as displayed in Fig. 3(b). This increasing trend continued for ϕ>2.35, whereas decrease of the concentration of degradation product was observed for ϕ<2.35, indicating that large value of rate constant is necessary to maintain high concentration inside cylindrical particle.

In Fig. 3(c), the concentration profile inside cylindrical particles is shown for various values of Thiele modulus, when dimensionless reaction time (τ) and bulk concentration (c_{r1}) are fixed as 0.3 and 0, respectively. Initial uniform concentration profile changed to concave shape due to simultaneous outward mass flux and generation of degradation component. Similar to spherical particles, maximum concentration at the center of the cylindrical particle increased with increasing value of ϕ, as shown in Fig. 3(c).

In this study, a slab-type PLGA particle surrounded by infinite medium was also modeled to predict c(r, τ) inside the particle by solving the reaction diffusion equation using eigenfunction expansion method. In rectangular coordinate, z was assumed as 0 in Eq. (1) under the same initial and boundary conditions in spherical or cylindrical particles. Similar to other geometries, mathematical solution, c(r, τ), was considered as the summation of transient and steady-state concentration, c(r, τ)=v(r, τ)+w(r). For each solution, the following differential equations should be established to satisfy the original reaction diffusion equation.

$$\frac{\partial v}{\partial \tau}=\frac{\partial^2 v}{\partial r^2}+\phi^2 v \text{ subject to } \left(\frac{\partial v}{\partial r}\right)_{r=0}=0,$$
$$v(1,\tau)=0, \text{ and } v(r,0)=c(r,0)-w(r) \quad (17)$$

$$\frac{d^2 w}{dr^2}+\phi^2 w=0 \text{ subject to } \left(\frac{dw}{dr}\right)_{r=0}=0 \text{ and } w(1)=c_{r1} \quad (18)$$

Steady-state solution can be solved as $w(r)=c_{r1}\frac{\cos(\phi r)}{\cos\phi}$ by solving ordinary differential Eq. (18), whereas transient solution can be obtained by solving Eq. (17) using eigenfunction expansion method. Once operator $\underline{L}$ and eigenfunction $K_n(r)$ can be defined as $\underline{L}=\frac{d^2}{dr^2}+\phi^2$ and $\underline{L}K_n=-\zeta_n^2 K_n$, respectively, $K_n(r)$ can be obtained by solving $\frac{d^2K_n}{dr^2}+\phi^2K_n=-\zeta_n^2K_n$ to satisfy boundary conditions such as $\left(\frac{dK_n}{dr}\right)_{r=0}=0$ and $K_n(1)=0$. Thus, transient solution, v(r, τ) can be expressed using the following eigenfunction expansion.

$$v(r,\tau)=\sum_{n=1}^{\infty}a_n(\tau)K_n(r)=\sum_{n=1}^{\infty}a_n(\tau)\cos(\lambda_n r) \quad (19)$$

Since Eq. (19) should satisfy Eq. (17), time dependent coefficient, $a_n(\tau)$ can be obtained by solving $\frac{da_n(\tau)}{d\tau}=-\zeta_n^2 a_n(\tau)$ to obtain $a_n(\tau)=a_n(0)\exp[(\phi^2-\lambda_n^2)\tau]$. Thus, detailed form of v(r, τ) can be derived as the following equations.

$$v(r,\tau)=\sum_{n=1}^{\infty}a_n(0)\cos(\lambda_n r)\exp[(\phi^2-\lambda_n^2)\tau] \quad (20)$$

$$v(r,0)=\sum_{n=1}^{\infty}a_n(0)\cos(\lambda_n r)=c_{t0}-c_{r1}\frac{\cos(\phi r)}{\cos\phi} \quad (21)$$

If $\phi\neq\lambda_n$, $a_n(0)$ can be obtained from Eq. (20) using orthogonality condition of eigenfunctions as the following manner.

$$a_n(0)=\frac{\langle v(r,0),\cos(\lambda_n r)\rangle}{\langle\cos(\lambda_n r),\cos(\lambda_n r)\rangle}=\frac{\frac{c_{t0}}{\lambda_n}\sin\lambda_n-\frac{c_{r1}}{2(\phi+\lambda_n)}\frac{\sin(\phi+\lambda_n)}{\cos\phi}-\frac{c_{r1}}{2(\phi-\lambda_n)}\frac{\sin(\phi-\lambda_n)}{\cos\phi}}{1/2} \quad (22)$$

Thus, the concentration inside slab-type particle can be expressed as the following equation.

$$c(r,\tau)=\frac{c_{r1}\cos(\phi r)}{\cos\phi}+2\sum_{n=1}^{\infty}\left[\frac{c_{t0}}{\lambda_n}\sin\lambda_n-\frac{c_{r1}}{2\cos\phi}\left\{\frac{\sin(\phi+\lambda_n)}{\phi+\lambda_n}+\frac{\sin(\phi-\lambda_n)}{\phi-\lambda_n}\right\}\right]\exp[(\phi^2-\lambda_n^2)\tau]\cos(\lambda_n r) \quad (23)$$

Average concentration of degradation product can be calculated by defining $\bar{c}(\tau)=\int_0^1 c(r,\tau)dr$, to yield the following result.

$$\bar{c}(\tau)=\frac{c_{r1}\tan(\phi r)}{\phi}+\sum_{n=1}^{\infty}\left[\frac{2c_{t0}}{\lambda_n}\sin\lambda_n-\frac{c_{r1}}{\cos\phi}\left\{\frac{\sin(\phi+\lambda_n)}{\phi+\lambda_n}+\frac{\sin(\phi-\lambda_n)}{\phi-\lambda_n}\right\}\right]\exp[(\phi^2-\lambda_n^2)\tau]\frac{\sin\lambda_n}{\lambda_n} \quad (24)$$

If $\phi=\lambda_n$, $a_n(0)$ can be calculated as the following simpler form.

$$a_n(0)=\frac{\langle v(r,0),\cos(\lambda_n r)\rangle}{\langle\cos(\lambda_n r),\cos(\lambda_n r)\rangle}=\frac{\frac{c_{t1}}{\lambda_n}\sin\lambda_n-\frac{c_{r1}}{2\cos\phi}}{1/2} \quad (25)$$

In this case, c(r, τ) and the average concentration can be expressed in the following manner.

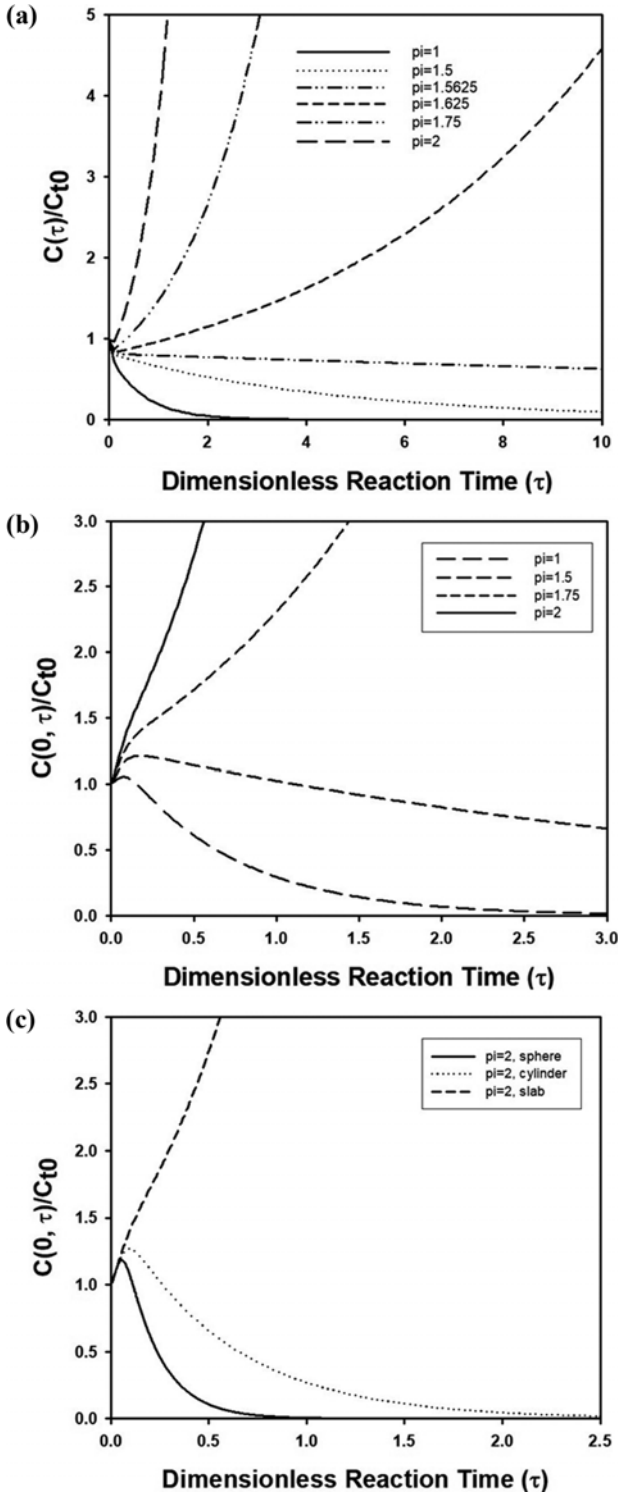

Fig. 4. Change of (a) dimensionless average concentration of degradation product inside slab-type PLGA particle and (b) dimensionless concentration of degradation product at the center of the slab-type PLGA particle as a function of dimensionless reaction time for various values of Thiele modulus. (c) Change of dimensionless concentration at the center of the three types of PLGA particles as a function of dimensionless reaction time for ϕ=2. The particles were modeled as immersed body in infinite medium, and the concentration of the product in the medium, C_{r1} was assumed as 0.

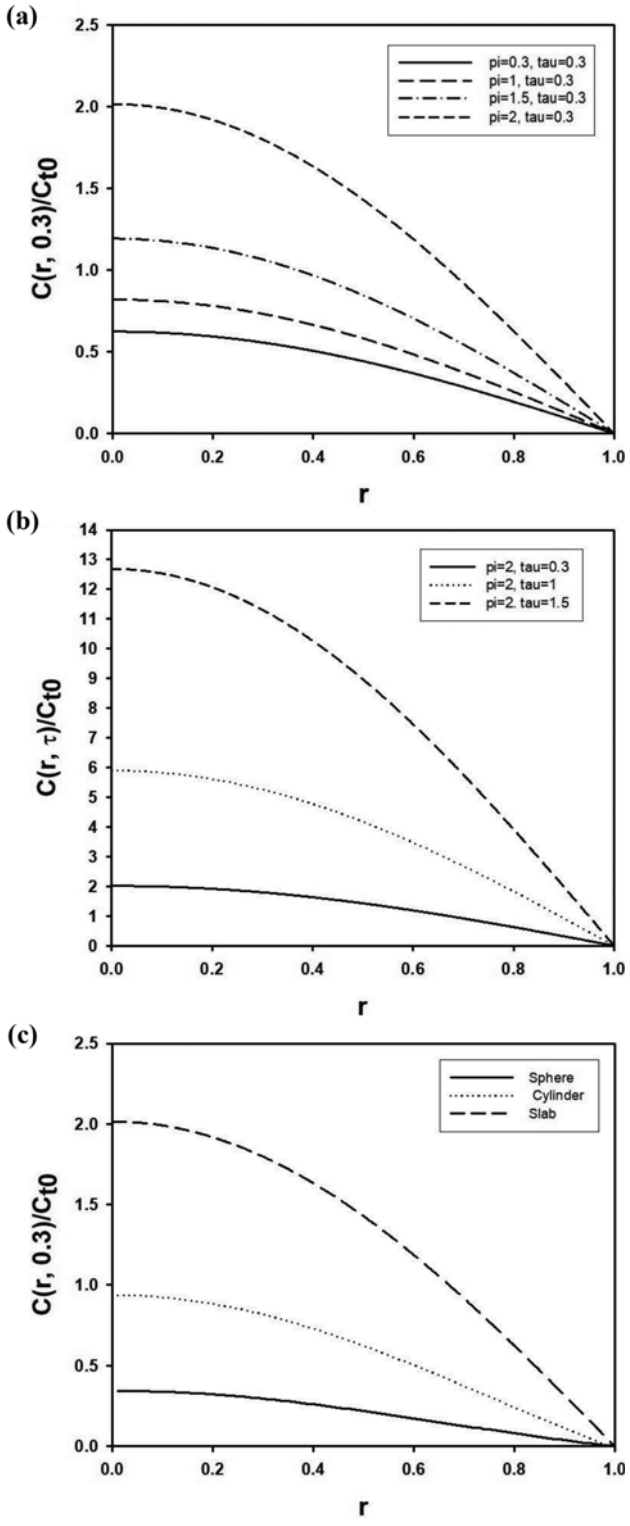

Fig. 5. Concentration profile of degradation product inside slab-type PLGA particle as a function of dimensionless radial distance from the center of the particle (a) for τ=0.3 and various values of ϕ and (b) for ϕ=2 and various values of τ. (c) Concentration profile of the degradation product inside three types of the particles for ϕ=2 and τ=0.3. The particles were modeled as immersed body in infinite medium, and the concentration of the product in the medium, C_{r1} was assumed as 0.

$$c(r,\ \tau)=\frac{c_{r1}\cos(\phi r)}{\cos\phi} + \sum_{n=1}^{\infty}\left(\frac{2c_{t0}}{\lambda_n}\sin\lambda_n-\frac{c_{r1}}{\cos\phi}\right)\exp[(\phi^2-\lambda_n^2)\tau]\cos(\lambda_n r) \quad (26)$$

$$\bar{c}(\tau)=\frac{c_{r1}\tan(\phi)}{\phi}+\sum_{n=1}^{\infty}\left(\frac{2c_{t0}}{\lambda_n}\sin\lambda_n-\frac{c_{r1}}{\cos\phi}\right)\exp[(\phi^2-\lambda_n^2)\tau]\frac{\sin\lambda_n}{\lambda_n} \quad (27)$$

Fig. 4(a) contains change of average concentration in slab-type particle as a function of dimensionless reaction time for various values of Thiele modulus ϕ and c_{r1}=0. When ϕ is smaller than 1.5625, the average concentration of degraded component decreases with reaction time, whereas the concentration increases after short decreasing period for $\phi\geq$1.625. On the contrary, concentration at the center of the slab-type particle showed maximum, when ϕ is smaller than 1.5, as displayed in Fig. 4(b). Further increase of Thiele modulus resulted in inflection point instead of maximum and consistent rise of concentration is observed with reaction time. In Fig. 4(c), change of concentration at the center is compared for spherical, cylindrical, and slab-type particles for the same value of ϕ=2. Since surface to volume ratio of spherical particles is larger than cylindrical or slab-type particles, decreasing rate of the concentration of degraded component was the most fast among three types of particles, indicating that outward mass flux of the generated component is much higher than generation rate.

Concentration profile inside a slab-type particle is shown in Fig. 5(a) for various values of Thiele modulus, when dimensionless reaction time τ and bulk concentration c_{r1} are fixed as 0.3 and 0, respectively. For every case, the concentration distribution is concave shape with maximum value at the center of the particle, and the concentration increases with increasing value of ϕ because of enhanced reaction rate. As demonstrated in Fig. 5(b), concentration increase is observed with increasing reaction time due to progression of the first order reaction, when ϕ is fixed as 2. In Fig. 5(c), concentration profiles inside particles with different geometries are also compared under the same reaction conditions such as ϕ=2 and τ=0.3. Similar to results in Fig. 4(c), the highest concentration of generated chemical species is predicted in a slab-type particle, since outward mass flux through the particle surface is not sufficient compared to generation rate of the degradation component in the slab-type particle.

2. Effect of *Biot* Number on Transient behavior of Concentration Change Inside PLGA Particle Immersed in Infinite Medium

In the previous section, the bulk concentration of degraded components at some instance was assumed as the same value as the concentration on particle surface immersed in infinite medium. However, this is not the general case, since mass transfer resistance inside particles is not the same as that in bulk medium. Thus, it is necessary to define the ratio of mass transfer resistance inside solid particles to bulk fluid phase as dimensionless group, *Biot* number, in the following manner.

$$Bi=\frac{k_L R}{D_e}=\frac{R/D_e}{1/k_L} \quad (28)$$

Here, k_L stands for mass transfer coefficient of degraded component between particle and surrounding bulk medium. To reflect the effect of *Biot* number, the boundary condition of Eq. (1) in spherical coordinates can be replaced as the following equation.

$$\text{Boundary conditions: } (\partial c/\partial r)_{r=0}=0 \text{ and } k_L\{c(1,t)-c_{r1}\}=-D/R(\partial c/\partial r)_{r=1} \quad (29)$$

By replacing $c(r,\ \tau)=v(r,\ \tau)/r$, the original differential equation in spherical coordinates can be changed to the following simpler form.

$$\frac{\partial v}{\partial\tau}=\frac{\partial^2 v}{\partial r^2}+\phi^2 v \text{ subject to } v(0,\ \tau)=0,\ \left(\frac{\partial v}{\partial r}\right)_{r=1}+(Bi-1)v(1,\ \tau)=Bic_{r1}, \text{ and } v(r,\ 0)=rc_{t0} \quad (30)$$

To solve the above equation, the solution can be divided as $v(r,\ \tau)=u(r,\ \tau)+w(r)$, followed by solving the unsteady and steady solution from the following equations.

$$\frac{\partial u}{\partial\tau}=\frac{\partial^2 u}{\partial r^2}+\phi^2 u \text{ subject to } u(0,\ \tau)=0,\ \left(\frac{\partial u}{\partial r}\right)_{r=1}+(Bi-1)u(1,\ \tau)=0, \text{ and } u(r,\ 0)=v(r,\ 0)-w(r) \quad (31)$$

$$\frac{d^2 w}{dr^2}+\phi^2 w=0 \text{ subject to } w(0)=0 \text{ and } \left(\frac{\partial w}{\partial r}\right)_{r=1}+(Bi-1)w(1,\ \tau)=Bic_{r1} \quad (32)$$

The solution of ordinary differential Eq. (32) can be found as $w(r)=\frac{Bi}{(Bi-1)\sin\phi+\phi\cos\phi}c_{r1}\sin(\phi r)$, and $u(r,\ \tau)$ can be expanded as $u(r,\ \tau)=\sum_{n=1}^{\infty}a_n(\tau)K_n(r)$ using eigenfunction, $K_n(r)$, and time dependent coefficient, $a_n(\tau)$. Since $K_n(r)$ satisfies $\nabla K_n(r)=-\zeta_n^2 K_n(r)$ subject

Table 1. Eigenvalues λ_n for various values of Bi, when spherical PLGA particle is immersed in infinite medium

Bi	λ_1	λ_2	λ_3	λ_4	λ_5	λ_6	λ_7
0.1	0.542	4.518	7.738	10.913	14.073	17.227	20.376
1.1	1.632	4.734	7.867	11.005	14.144	17.285	20.425
10	2.836	5.717	8.659	11.653	14.687	17.748	20.828
15	2.935	5.885	8.861	11.863	14.892	17.941	21.008
20	2.986	5.978	8.983	12.003	15.038	18.089	21.152
30	3.037	6.077	9.12	12.169	15.225	18.287	21.356
100	3.11	6.22	9.331	12.441	15.552	18.663	21.775
1,000	3.138	6.277	9.415	12.554	15.692	18.831	21.969
∞	3.1416	6.2832	9.4248	12.5664	15.7080	18.8496	21.9911

to $K_n(0)=0$ and $\left(\frac{dK_n}{dr}\right)_{r=1}+(Bi-1)K_n(1)=0$, $K_n(r)$ can be found as $\sin(\lambda_n r)$, where eigenvalues, λ_n satisfy the eigenvalue equation, $\frac{\lambda_n}{1-Bi}=\tan\lambda_n$. Here, λ_n is defined as $\lambda_n^2=\phi^2+\xi_n^2$, and can be computed by solving the transcendental eigenvalue equation after fixing *Biot* number, as shown in Table 1. The digits in the last row from the table also show eigenvalues for $Bi\to\infty$, which was obtained by solving $\sin\lambda_n=0$ or $\lambda_n=n\pi$ (n=1, 2, 3, …).

By substituting eigenfunction expansion of $u(r,\tau)$ to Eq. (31) and applying the relationship, $\underline{\underline{L}}K_n(r)=-\zeta_n^2K_n(r)$, $a_n(\tau)$ can be found from the following relationship.

$$\sum_{n=1}^{\infty}\frac{da_n(\tau)}{d\tau}\sin(\lambda_n r)=\sum_{n=1}^{\infty}(\phi^2-\lambda_n^2)\sin(\lambda_n r) \tag{33}$$

Thus, $a_n(\tau)$ can be solved as $a_n(\tau)=a_n(0)\exp\{(\phi^2-\lambda_n^2)\tau\}$, and $a_n(0)$ can be obtained by applying orthogonality condition of eigenfunctions to obtain $a_n(\tau)$ as the following manner for $\phi\neq\lambda_n$.

$$a_n(\tau)=\frac{\langle v(r,0)-w(r),\sin(\lambda_n r)\rangle}{\langle\sin(\lambda r),\sin(\lambda_n r)\rangle} \tag{34}$$

$$=\frac{c_{t0}\left(-\frac{\cos\lambda_n}{\lambda_n}+\frac{\sin\lambda_n}{\lambda_n^2}\right)+\frac{1}{2}\left\{\frac{\sin(\phi+\lambda_n)}{\phi+\lambda_n}-\frac{\sin(\phi-\lambda_n)}{\phi-\lambda_n}\right\}\frac{Bic_{r1}}{(Bi-1)\sin\phi+\phi\cos\phi}}{\frac{1}{2}-\frac{\sin(2\lambda_n)}{4\lambda_n}}$$

When ϕ equals to λ_n, $a_n(\tau)$ can be obtained as the following equation.

$$a_n(\tau)=\frac{c_{t0}\left(-\frac{\cos\lambda_n}{\lambda_n}+\frac{\sin\lambda_n}{\lambda_n^2}\right)-\left(\frac{1}{2}-\frac{\sin(2\lambda_n)}{4\lambda_n}\right)\frac{Bic_{r1}}{(Bi-1)\sin\phi+\phi\cos\phi}}{\frac{1}{2}-\frac{\sin(2\lambda_n)}{4\lambda_n}} \tag{35}$$

Thus, the concentration of degraded components can be expressed as a function of r, τ, and Bi, using the following equation.

$(\phi\neq\lambda_n)$

$$c(r,\tau)=$$

$$\sum_{n=1}^{\infty}\frac{c_{t0}\left(-\frac{\cos\lambda_n}{\lambda_n}+\frac{\sin\lambda_n}{\lambda_n^2}\right)+\frac{1}{2}\left\{\frac{\sin(\phi+\lambda_n)}{\phi+\lambda_n}-\frac{\sin(\phi-\lambda_n)}{\phi-\lambda_n}\right\}\frac{Bic_{r1}}{(Bi-1)\sin\phi+\phi\cos\phi}}{\frac{1}{2}-\frac{\sin(2\lambda_n)}{4\lambda_n}}$$

$$\frac{\sin(\lambda_n r)}{r}\exp\{(\phi^2-\lambda_n^2)\tau\}+\frac{Bic_{r1}}{(Bi-1)\sin\phi+\phi\cos\phi}\frac{\sin(\phi r)}{r} \tag{36}$$

$(\phi=\lambda_n)$

$$c(r,\tau)=$$

$$\sum_{n=1}^{\infty}\frac{c_{t0}\left(-\frac{\cos\lambda_n}{\lambda_n}+\frac{\sin\lambda_n}{\lambda_n^2}\right)-\left\{\frac{1}{2}-\frac{\sin(2\lambda_n)}{4\lambda_n}\right\}\frac{Bic_{r1}}{(Bi-1)\sin\phi+\phi\cos\phi}}{\frac{1}{2}-\frac{\sin(2\lambda_n)}{4\lambda_n}}$$

$$\frac{\sin(\lambda_n r)}{r}\exp\{(\phi^2-\lambda_n^2)\tau\}+\frac{Bic_{r1}}{(Bi-1)\sin\phi+\phi\cos\phi}\frac{\sin(\phi r)}{r} \tag{37}$$

Thus, the average concentration inside spherical particles immersed

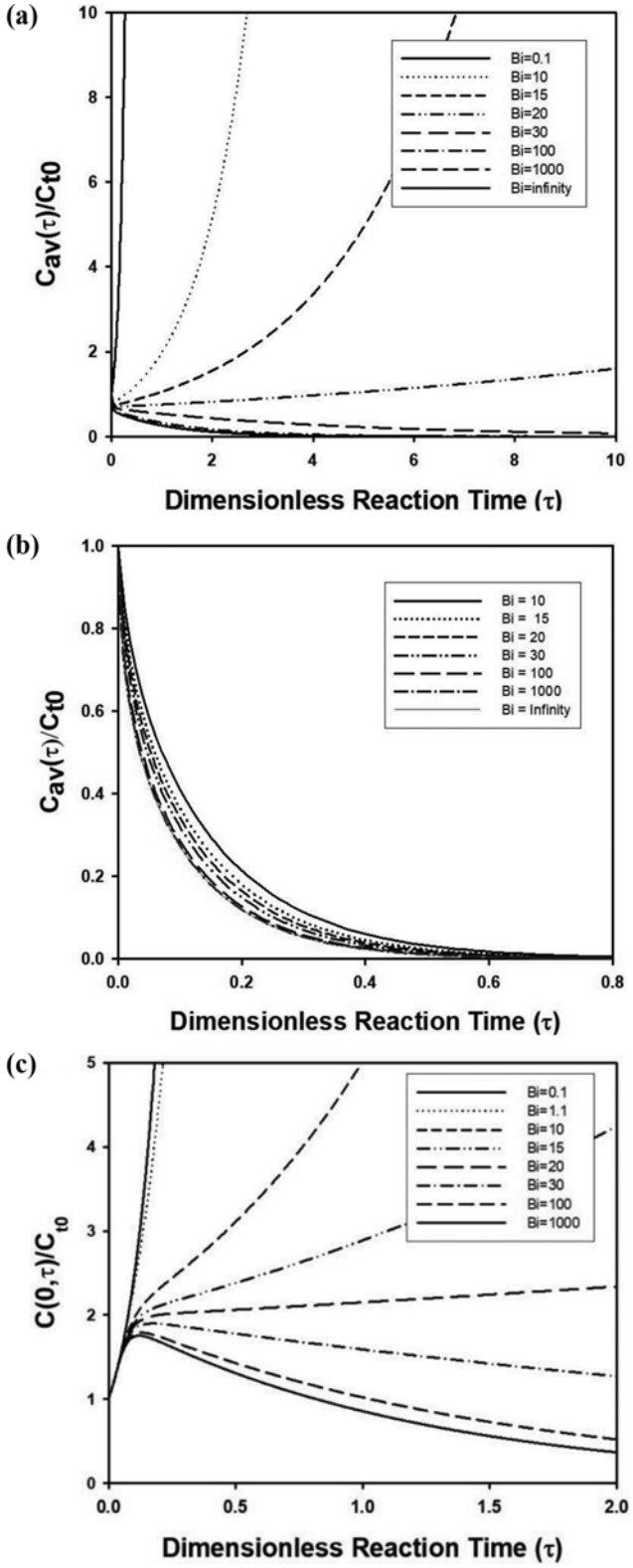

Fig. 6. Change of average concentration of degraded component inside spherical PLGA particle surrounded in infinite medium as a function of dimensionless reaction time for various values of *Biot* number and (a) ϕ=3 and (b) ϕ=1.3. (c) concentration change at the center of spherical particle surrounded in infinite medium as a function of dimensionless reaction time for various values of *Biot* number. ϕ was assumed as 3.

in infinite medium can be also obtained as a function of τ and Bi by integration. For this purpose, it is convenient to use $3\int_0^1 r^2\frac{\sin(\lambda_n r)}{r}dr = 3\left(\frac{\sin\lambda_n}{\lambda_n^2}-\frac{\cos\lambda_n}{\lambda_n}\right)$ and $3\int_0^1 r^2\frac{\sin(\phi r)}{r}dr = 3\left(\frac{\sin\phi}{\phi^2}-\frac{\cos\phi}{\phi}\right)$. Concentration at the center of the spherical particle can be also computed by applying L'Hospital's theorem to Eqs. (36) and (37).

Fig. 6(a) contains the change of average dimensionless concentration of degraded components inside a spherical particle as a function of dimensionless reaction time for fixed value of Thiele modulus, ϕ=3 and various values of *Biot* number from 0.1 to 1,000. Unlike Fig. 2(a), the concentration changed drastically depending on the value of *Biot* number. As *Bi* decreased from 1,000 to 30, the decreasing rate of the concentration became smaller, since mass transfer resistance in surrounding liquid medium increased, causing accumulation of degraded components inside particles. When *Bi* was smaller than 20, transient behavior of the concentration was an increasing trend rather than decreasing, implying that drastic increase of the concentration of degraded component can be expected for ϕ=3, unlike the result for the same value of Thiele modulus in Fig. 2(a). Since the results shown in Fig. 2(a) were computed by assuming the same concentration in bulk medium as the concentration of the particle surface, it can be obtained by setting *Biot* number as an infinite value. In Fig. 6(a), the concentration change was computed and compared with the result for Bi→∞, which was almost the same to the case of Bi=1,000. When ϕ was reduced to 1.3 in Fig. 6(b), decreasing trends of the concentration were similar for the results with various values of *Biot* number, implying that there was little effect of *Biot* number because of decrease of reaction rate and particle size, or increase of diffusion coefficient.

For comparison, the concentration of degraded components as average value in Fig. 6(a) was compared with the concentration at the center of the particles, when Thiele modulus was kept as the same value (ϕ=0.3). Fig. 6(c) contains the concentration of degraded components at the center of spherical particles surrounded in infinite medium. For computation, ϕ was fixed as 0.3, while Bi was varied from 0.1 to 1,000. Similar to the average concentration shown in Fig. 6(a), decreasing rate of the concentration became faster, as Bi increased from 30 to 1,000. When Bi was larger than 20, the concentration increased with increasing reaction time, and the increasing rate became much faster, as Bi decreased from 20 to 0.1. Since the resistance of mass transfer of surrounding medium can be considered as a large value for very small *Bi*, drastic increase of the concentration was predicted for Bi=0.1, as shown in Fig. 6(c).

Though the reaction-diffusion equation with *Biot* number as variable parameter can be solved numerically using commercial software, analytical solution can be a significant result, because a rigorous solution can be obtained using analytical method to provide better understanding of transport phenomena without relying on a numerical approach. However, concentration profiles inside a spherical particle as a function of dimensionless reaction time were plotted for various values of *Biot* number and fixed value of ϕ=2, using commercial software, MATLAB, because of excellent visualization function in 3D graphics. For calculation, 'pdepe' command was used combined with m-file for definition of governing equation and boundary condition for adjustment of *Biot* number and ϕ. As shown In Fig. 7(a), abrupt rise of concentration of degraded components near the center of the spherical particle was predicted, whereas the concentration decreased near the particle surface after initiation of the reaction for Bi=2. Though the decreasing rate of the concentration was slow for small value of Bi, it decayed

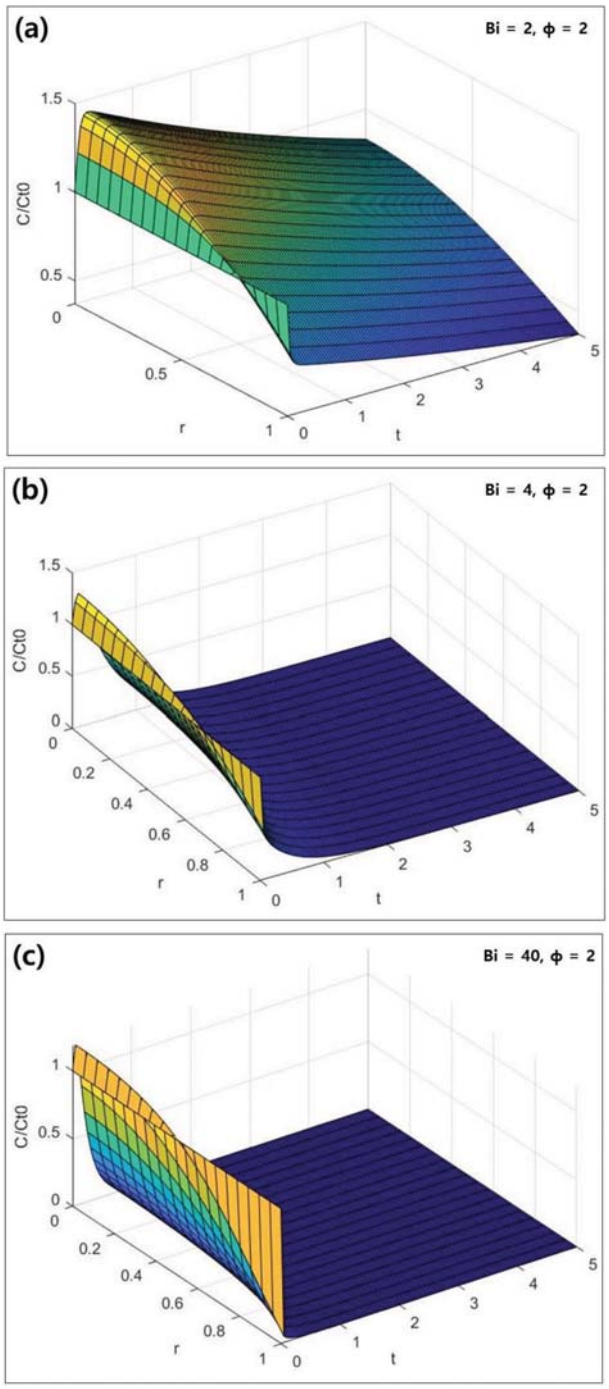

Fig. 7. Change of concentration profile inside spherical particle immersed in infinite medium as a function of dimensionless reaction time. Bi and ϕ were fixed as (a) 2 and 2, (b) 4 and 2, and (c) 40 and 2, respectively.

rapidly as *Biot* number increased to 4 or 40, which is demonstrated in Fig. 7(b) and 7(c).

In addition to spherical particles, the effect of *Biot* number on the concentration change of degradation product was studied for cylindrical or slab-type particles surrounded in infinite medium. In cylindrical and slab-type particles, the second boundary condition at particle surface can be written as the following equations.

(For cylinder and slab)

$$\left(\frac{\partial c}{\partial r}\right)_{r=1} + \mathrm{Bi}c(1,\ \tau) = \mathrm{Bi}c_{r1} \tag{38}$$

By dividing the solution as $c(r,\ \tau)=u(r,\ \tau)+w(r)$, the unsteady and steady solution can be found as the mathematical form to satisfy homogeneous and nonhomogeneous boundary condition at particle surface, respectively. Since the approach to solve reaction-diffusion equation in cylindrical or cartesian coordinate by eigenfunction expansion method considering *Biot* number is similar to the case in spherical particles, the following solutions can be obtained as function of r and τ without detailed procedures.

(For cylinder)

$$c(r,\ \tau)=$$
$$2\sum_{n=1}^{\infty}\frac{c_{t0}\dfrac{\mathrm{Bi}^2}{\lambda_n}-\dfrac{\mathrm{Bi}c_{r1}}{\mathrm{Bi}J_0(\phi)+\phi J_1(\phi)}\dfrac{\lambda_n J_1(\phi)}{\lambda_n+\phi}}{(\lambda_n^2+\mathrm{Bi}^2)J_1(\lambda_n)}J_0(\lambda_n r)\exp\{(\phi^2-\lambda_n^2)\tau\}$$
$$+\frac{\mathrm{Bi}c_{r1}}{\mathrm{Bi}J_0(\phi)-\phi J_1(\phi)}J_0(\phi r) \tag{39}$$

(For slab, $\phi\neq\lambda_n$)

$$c(r,\ \tau)=$$
$$2\sum_{n=1}^{\infty}\frac{c_{t0}\dfrac{\sin\lambda_n}{\lambda_n}-\dfrac{1}{2}\dfrac{\mathrm{Bi}c_{r1}}{\mathrm{Bi}\cos\phi-\phi\sin\phi}\left\{\dfrac{\sin(\phi+\lambda_n)}{\phi+\lambda_n}+\dfrac{\sin(\phi-\lambda_n)}{\phi-\lambda_n}\right\}}{\dfrac{1}{2}+\dfrac{\sin(2\lambda_n)}{4\lambda_n}}$$
$$\cos(\lambda_n r)\exp\{(\phi^2-\lambda_n^2)\tau\}+\frac{\mathrm{Bi}c_{r1}}{\mathrm{Bi}\cos\phi-\phi\sin(\phi)}\cos(\phi r)$$

(For slab, $\phi=\lambda_n$)

$$c(r,\ \tau)=$$
$$2\sum_{n=1}^{\infty}\frac{c_{t0}\dfrac{\sin\lambda_n}{\lambda_n}-\dfrac{1}{2}\dfrac{\mathrm{Bi}c_{r1}}{\mathrm{Bi}\cos\phi-\phi\sin\phi}\left\{\dfrac{1}{2}+\dfrac{\sin(2\lambda_n)}{4\lambda_n}\right\}}{\dfrac{1}{2}+\dfrac{\sin(2\lambda_n)}{4\lambda_n}}$$
$$\cos(\lambda_n r)\exp\{(\phi^2-\lambda_n^2)\tau\}+\frac{\mathrm{Bi}c_{r1}}{\mathrm{Bi}\cos\phi-\phi\sin(\phi)}\cos(\phi r) \tag{40}$$

In the above solutions, eigenvalues, λ_n can be found by solving the following transcendental equations, which were be derived from eigenvalue problems, $\underline{\underline{L}}K_n=-\xi_n^2K_n$.

(For cylinder) $\mathrm{Bi}J_0(\lambda_n)=\lambda_n J_1(\lambda_n)$ (41)

(For slab) $\lambda_n=\mathrm{Bi}\cot\lambda_n$ (42)

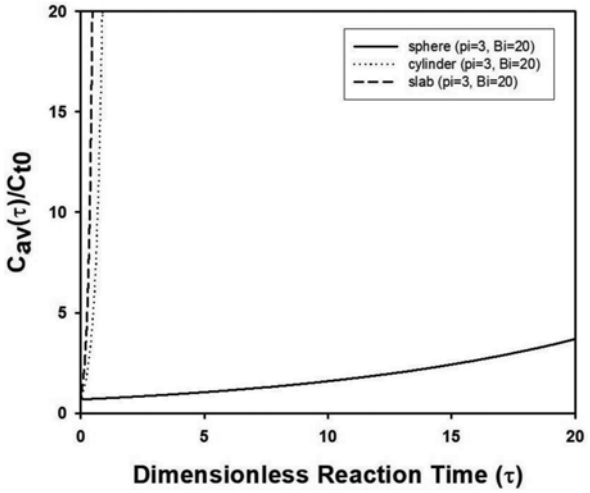

Fig. 8. Change of average concentration of degraded component inside PLGA particles with various morphologies immersed in infinite medium as a function of dimensionless rection time for Bi=20 and ϕ=3.

In cylindrical coordinates, the average concentration inside particle can be found as a function of τ and Bi after integration, $2\int_0^1 rJ_0(\lambda_n r)dr = 2\left[\frac{r}{\lambda_n}J_1(\lambda_n r)\right]_{r=0}^{r=1} = \frac{2}{\lambda_n}J_1(\lambda_n)$ and $2\int_0^1 rJ_0(\phi r)dr = \frac{2}{\phi}J_1(\phi)$. Similarly, the average concentration inside slab-type particles can be calculated after integration, $\int_0^1\cos(\lambda_n r)dr=\frac{\sin\lambda_n}{\lambda_n}$ and $\int_0^1\cos(\phi r)dr=\frac{\sin\phi}{\phi}$.

Fig. 8 contains the change of average concentration of degraded components as a function of dimensionless reaction time. The computation was carried out for spherical, cylindrical, and slab-type particles immersed in infinite medium under the same reaction conditions such as ϕ=3 and Bi=20 applying eigenvalues listed in Table 2. Though increasing trend was observed for each particle, the generation rate inside spherical particles was quite slow, compared to other particle geometries. Slab-type particles showed the most rapid increasing rate of the concentration, since the smallest surface area caused the accumulation of degraded component.

3. Coupled Differential Equation for Prediction of Bulk and Transient Concentration Inside Particles with Various Morphologies Immersed in Finite Medium

In a real experiment, fixed amount of porous spherical PLGA particles with radius R can be immersed in reaction system with finite volume, V. Such particles can be synthesized by double emulsion system using various biodegradable polymers such as PLGA, PLA, and PCL [22]. In this situation, the concentration of generated

Table 2. Eigenvalues λ_n for ϕ=3 and Bi=20, when cylindrical or slab-type PLGA particle is immersed in infinite medium

	λ_1	λ_2	λ_3	λ_4	λ_5	λ_6	λ_7
Cylinder	2.288	5.257	8.253	11.268	14.298	17.344	20.404
Slab	1.496	4.491	7.495	10.512	13.542	16.586	19.644

component in bulk medium cannot be considered as constant value as in the previous section. Thus, it is necessary to consider material balances in particles and bulk fluid phase simultaneously to obtain the following coupled differential equations.

$$\varepsilon_p\frac{\partial c_p}{\partial t}=D_e\frac{1}{\hat{r}^2}\frac{\partial}{\partial \hat{r}}\left(\hat{r}^2\frac{\partial c_p}{\partial \hat{r}}\right)+kc_p$$

$$\text{subject to } c_p(\hat{r},\ \tau)=c_{t0},\ \left(\frac{\partial c_p}{\partial \hat{r}}\right)_{\hat{r}=0}=0 \text{ and } c_p(R,\ t)=c_b(t) \tag{43}$$

$$\frac{dc_b}{dt}=-\frac{1}{V}\frac{m_p}{\rho_p}\frac{3}{R}D_e\left(\frac{\partial c_p}{\partial r}\right)_{\hat{r}=R} \text{ subject to } c_b(0)=0 \tag{44}$$

Here, m_p and ρ_p indicate mass and density of PLGA particles with void fraction, ε_p, suspended in liquid medium. In the above equation, the initial concentration of degradation product in bulk phase was set to zero and a uniform profile of initial concentration inside particles was assumed to obtain transient concentration in particles, $c_p(\hat{r},\ t)$ and in bulk phase, $c_b(t)$ as a function of radial distance, $\hat{r}$ and reaction time, t. Since bulk concentration was assumed as the same value as the surface concentration on PLGA particles, *Biot* number was regarded as infinite for simplicity of modeling. When the above differential equations satisfy the initial and boundary conditions shown in Eqs. (43) and (44), the following non-dimensionalization is possible by defining dimensionless radial distance, r, characteristic time, t_c, and Thiele modulus, ϕ^2 as $\frac{\hat{r}}{R}$, $\frac{R^2}{D_e}\varepsilon_p$, and $\frac{kR^2}{D_e}\varepsilon_p$, respectively.

$$\frac{\partial y_b}{\partial \tau}=\frac{1}{r^2}\frac{\partial}{\partial r}\left(r^2\frac{\partial y_p}{\partial r}\right)+\phi^2 y_p \text{ (for sphere)}$$

$$\text{subject to } y_p(r,\ 0)=1,\ \left(\frac{\partial y_p}{\partial x}\right)_{r=0}=0 \text{ and } y_p(1,\ \tau)=y_b(\tau) \tag{45}$$

$$\frac{dy_b}{d\tau}=-\frac{3\varepsilon_p}{V}\frac{m_p}{\rho_p}\left(\frac{\partial y_p}{\partial x}\right)_{r=1} \text{ subject to } y_b(0)=0 \tag{46}$$

To solve the above differential equation, Laplace transform was carried out to yield the following ordinary differential equations in Laplace domain.

$$sY_p(r,\ s)-1=\frac{1}{r^2}\frac{d}{dr}\left(r^2\frac{dY_p}{dr}\right)+\phi^2 Y_p=0$$

$$\text{subject to } \left(\frac{dY_p}{dr}\right)_{r=0}=0 \text{ and } Y_p(1,\ s)=Y_b(s) \tag{47}$$

$$sY_b(s)=-3\frac{m_p/\rho_p}{V}\varepsilon_p\left(\frac{\partial Y_p}{\partial r}\right)_{r=0} \tag{48}$$

$Y_p(r,\ s)$ and $Y_b(s)$ can be solved separately using undetermined coefficient, A(s).

$$Y_p(r,\ s)=A(s)\frac{\sin(i\sqrt{s-\phi^2}\cdot r)}{r}+\frac{1}{s-\phi^2}$$

$$\text{and } Y_b(s)=3\frac{m_p/\rho_p}{V}\varepsilon_p\frac{A(s)}{s}[\sin(i\sqrt{s-\phi^2})-i\sqrt{s-\phi^2}\cos(i\sqrt{s-\phi^2})] \tag{49}$$

Using the second boundary condition in Eq. (45) and Eq. (47), A(s) can be found as the following result, where i stands for imaginary number, $(-1)^{1/2}$.

$$A(s)=\frac{s}{s-\phi^2}\frac{1}{3\frac{m_p/\rho_p}{V}\varepsilon_p\{\sin(i\sqrt{s-\phi^2})-i\sqrt{s-\phi^2}\cos(i\sqrt{s-\phi^2})\}-s\cdot\sin(i\sqrt{s-\phi^2})} \tag{50}$$

Thus, transient concentration inside particles and bulk concentration can be derived separately in Laplace domain as the following equations.

$$Y_p(r,\ s)=\frac{1}{r}\frac{s}{s-\phi^2}\frac{\sin(i\sqrt{s-\phi^2}\cdot r)}{3\frac{m_p/\rho_p}{V}\varepsilon_p\{\sin(i\sqrt{s-\phi^2})-i\sqrt{s-\phi^2}\cos(i\sqrt{s-\phi^2})\}-s\cdot\sin(i\sqrt{s-\phi^2})}+\frac{1}{s-\phi^2} \text{ and}$$

$$Y_b(s)=-\frac{1}{s-\phi^2}\frac{3\frac{m_p/\rho_p}{V}\varepsilon_p\{(i\sqrt{s-\phi^2})\cos(i\sqrt{s-\phi^2})-\sin(i\sqrt{s-\phi^2})\}}{3\frac{m_p/\rho_p}{V}\varepsilon_p\{\sin(i\sqrt{s-\phi^2})-i\sqrt{s-\phi^2}\cos(i\sqrt{s-\phi^2})\}-s\cdot\sin(i\sqrt{s-\phi^2})} \tag{51}$$

Since $y_p(r,\ \tau)$ and $y_b(\tau)$ can be found by inverse transform of the above equations, it is necessary to find poles to apply residue theorem. Thus, the following differential operator $\underline{\underline{L}}$ can be defined as

Table 3. Eigenvalues λ_n for various values of ϕ and $B=\frac{m_p/\rho_p}{V}\varepsilon_p$ of coupled differential equations of PLGA degradation system containing spherical PLGA particles

B	ϕ	λ_1	λ_2	λ_3	λ_4	λ_5	λ_6	λ_7
	0.01	0.0099	3.17	6.297	9.434	12.574	18.854	21.995
	0.1	0.057	0.099	3.17	6.297	9.434	12.574	15.714
0.03	1	0.984	3.173	6.298	9.434	12.574	15.714	18.854
	1.5	1.474	3.178	6.298	9.435	12.574	15.714	18.854
	2	1.959	3.187	6.299	9.435	12.574	15.714	18.854
0.1	1.5	1.419	3.254	6.333	9.457	12.59	15.727	18.866
0.15	1.5	1.385	3.303	6.357	9.473	12.602	15.737	18.874
0.3	1.5	1.474	3.178	6.298	9.435	12.574	15.714	18.854

matrix form to obtain eigenfunction $\underline{K_n}$ as vector form to define eigenvalue problem, $\underline{\underline{L}}\underline{K_n}=-\xi_n^2\underline{K_n}$.

$$\underline{\underline{L}}=\begin{bmatrix} \frac{1}{r^2}\frac{d}{dr}\left(r^2\frac{d}{dr}\right)+\phi^2 & 0 \\ -3\frac{m_p/\rho_p}{V}\varepsilon_p\left(\frac{d}{dr}\right)_{r=1} & 0 \end{bmatrix} \text{ and } \underline{K_n}=\begin{bmatrix} K_n(r) \\ D_n \end{bmatrix} \tag{52}$$

Since $K_n(r)$ satisfies $\left(\frac{dK_n(r)}{dr}\right)_{r=0}=0$ and $D_n=K_n(1)$, $K_n(r)$ and D_n can be determined as $K_n(x)=\frac{\sin(\lambda_n x)}{x}$ and $\sin\lambda_n$, respectively, when eigenvalue λ_n is defined as $\lambda_n^2=\xi_n^2+\phi^2$. Numerical values of λ_n can be computed by solving the following transcendental equation, and the digits are summarized in Table 3.

$$3\frac{m_p/\rho_p}{V}\varepsilon_p(\sin\lambda_n-\lambda_n\cos\lambda_n)+(\lambda_n^2-\phi^2)\sin\lambda_n=0 \tag{53}$$

In the above equation, the value of λ_n can be affected by reaction conditions such as Thiele modulus ϕ and $\frac{m_p/\rho_p}{V}\varepsilon_p$ in closed system. From Eq. (53), poles in Eq. (51) can be determined as $s_n=i\sqrt{\phi^2-\lambda_n^2}$ or $s=\phi^2$ to apply residue theorem and obtain $y_p(r,\tau)$ and $y_b(\tau)$, as the following mathematical solutions.

$$y_b(\tau)=\sum_{n=1}^{\infty}\frac{2\left(\frac{\phi^2-\lambda_n^2}{\lambda_n^2}\right)\left(3\frac{m_p/\rho_p}{V}\varepsilon_p\right)\exp\{(\phi^2-\lambda_n^2)\tau\}}{\left(3\frac{m_p/\rho_p}{V}\varepsilon_p\right)^2+\left(3\frac{m_p/\rho_p}{V}\varepsilon_p\right)\frac{2\lambda_n^2-\phi^2}{\lambda_n^2}+\frac{(\phi^2-\lambda_n^2)^2}{\lambda_n^2}} \tag{54}$$

$$\bar{y}_p(\tau)=3\sum_{n=1}^{\infty}\frac{2\left(\frac{\phi^2-\lambda_n^2}{\lambda_n^2}\right)^2\exp\{(\phi^2-\lambda_n^2)\tau\}}{\left(3\frac{m_p/\rho_p}{V}\varepsilon_p\right)^2+\left(3\frac{m_p/\rho_p}{V}\varepsilon_p\right)\frac{2\lambda_n^2-\phi^2}{\lambda_n^2}+\frac{(\phi^2-\lambda_n^2)^2}{\lambda_n^2}} \tag{55}$$

$$y_p(r,\tau)=\sum_{n=1}^{\infty}\frac{2\frac{m_p/\rho_p}{V}\varepsilon_p\frac{\phi^2-\lambda_n^2}{\lambda_n^2}\frac{\sin(\lambda_n x)}{x}\exp\{(\phi^2-\lambda_n^2)\tau\}}{\left\{\left(3\frac{m_p/\rho_p}{V}\varepsilon_p\right)^2+\left(3\frac{m_p/\rho_p}{V}\varepsilon_p\right)\frac{2\lambda_n^2-\phi^2}{\lambda_n^2}+\frac{(\phi^2-\lambda_n^2)^2}{\lambda_n^2}\right\}\sin\lambda_n} \tag{56}$$

In the above equations, $\bar{y}_p(\tau)$ is the average concentration of degraded component inside particles, which is defined as $\bar{y}_p(\tau)=3\int_0^1 r^2 y_p(r,\tau)dr$ in spherical coordinate. Fig. 9(a) contains the change of bulk concentration of degraded components, $y_b(\tau)$ as a function of dimensionless reaction time for various values of ϕ, when diluted suspension of spherical PLGA particles was assumed in batch medium ($B=\frac{m_p/\rho_p}{V}\varepsilon_p=0.03$). When ϕ is larger than 0.1, bulk concentration increased as a function of reaction time, and the

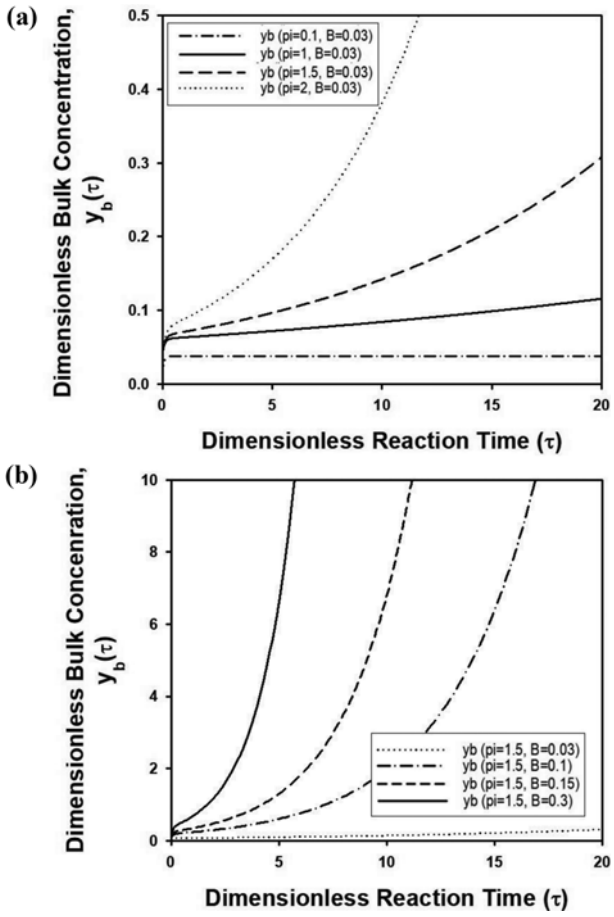

Fig. 9. Change of bulk concentration of degradation product, $y_b(\tau)$ in liquid medium with finite volume, V, containing spherical PLGA particles as a function of dimensionless reaction time (a) for $B=\frac{m_p/\rho_p}{V}\varepsilon_p=0.03$ and various values of ϕ and (b) for $\phi=1.5$ and various values of *B*. Initial concentration of the degradation product in surrounding medium was assumed as 0.

increasing rate became faster with increasing value of ϕ due to enhanced reaction rate. When ϕ reduced to 0.1, the bulk concentration increased rapidly in the initial stage of the reaction, finally reaching saturated value due to balancing of uptaking rate of the degraded component from the suspended particles and generation rate of the product. The effect of the amount of PLGA particles added in the liquid medium was also investigated by fixing $\phi=1.5$, while B was adjusted from 0.03 to 0.3, as shown in Fig. 9(b). Compared to diluted suspension (B=0.03), drastic increase of bulk concentration was observed from a more concentrated system (B>0.1), since mass flow rate from the PLGA particles to bulk medium increased when number density of the particles increased in concentrated system.

In addition to bulk concentration, average concentration inside particles was also plotted in Fig. 10(a), where ϕ was changed from 0.01 to 2 for fixed value of B=0.03 in diluted suspension. After short decreasing period in initial stage of reaction due to insufficient accumulation of the degraded component in spherical particles,

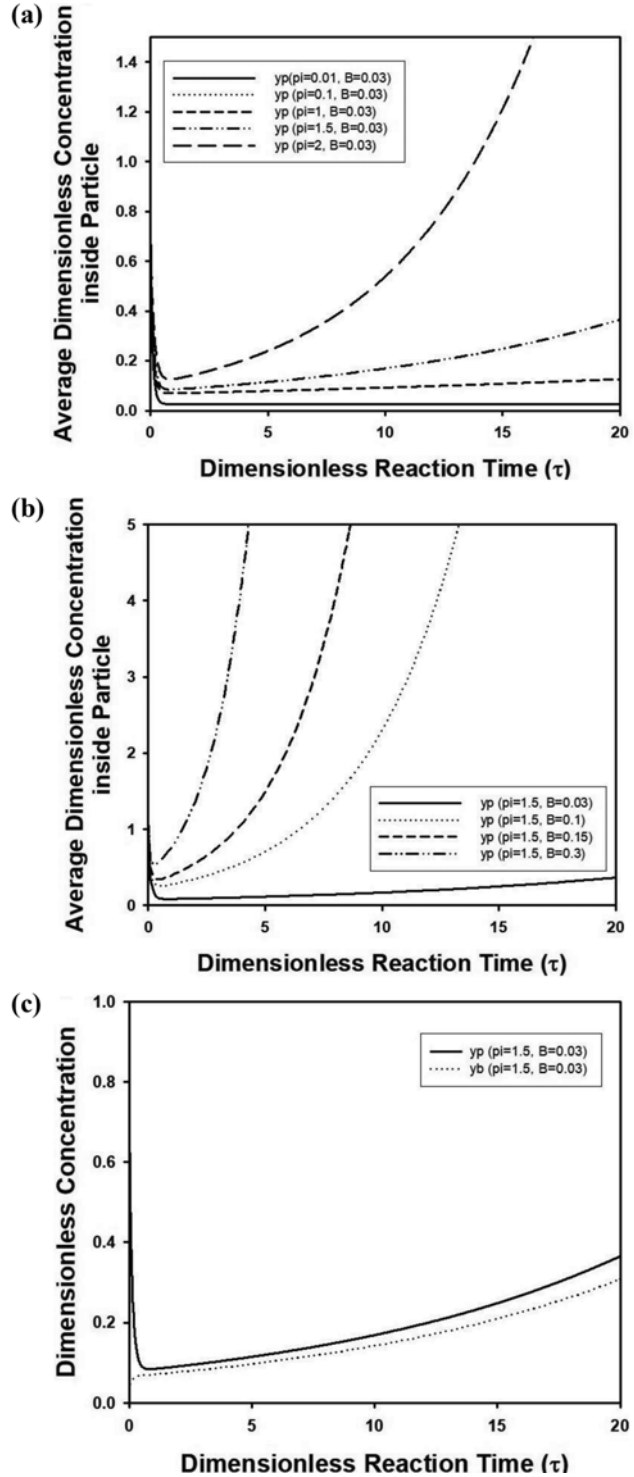

Fig. 10. Change of average dimensionless concentration of degradation product inside spherical particles, $\bar{y}_p(\tau)$ in liquid medium with finite volume, V, as a function of dimensionless reaction time (a) for B=$\frac{m_p/\rho_p}{V}\varepsilon_p$=0.03 and various values of ϕ and (b) for ϕ=1.5 and various values of B. (c) Change of $\bar{y}_p(\tau)$ inside spherical particles and $y_b(\tau)$ in surrounding medium with finite volume, V for ϕ=1.5 and B=0.03. Initial concentration of the degradation product in surrounding medium was assumed as 0.

the concentration increased with different rate depending on the value of ϕ. When ϕ was 0.01, concentration remained as almost constant value, while rapid increase was observed for the system with ϕ=2, implying that rate constant was large enough to compensate outward flux to bulk medium. The effect of the amount of suspended particles on the concentration of degraded product is plotted in Fig. 10(b) for fixed value of ϕ=1.5. Since the volume of the surrounding medium is finite as fixed value of V, mass flow rate of the degraded species from the spherical particles to bulk medium can be restricted, causing increase of $\bar{y}_p(\tau)$ with increasing value of the particle concentration, B. Similar to Fig. 10(a), initial decreasing period was observed for every reaction condition, whereas rising speed of the concentration increased with increasing value of volume fraction of the particle, B. When ϕ and B were fixed as 1.5 and 0.03, bulk concentration and average concentration inside particle were compared in Fig. 10(c), showing that $\bar{y}_p(\tau)$ was always higher than $y_b(\tau)$, causing outward mass flux of the degraded component.

In this study, an autocatalytic reaction system with suspended cylindrical particles in finite medium was also modeled to predict bulk concentration in surrounding liquid and average concentration inside the particles as a function of reaction time. Assuming initial concentration in bulk liquid, c_{r1} was 0, the following governing equations were derived for dimensionless concentrations, $\bar{y}_p(\tau)$ and $y_b(\tau)$.

$$\frac{\partial y_p}{\partial \tau}=\frac{1}{r}\frac{\partial}{\partial r}\left(r\frac{\partial y_p}{\partial r}\right)+\phi^2 y_p \text{ (for cylinder)}$$

$$\text{subject to } y_p(r,0)=1,\left(\frac{\partial y_p}{\partial r}\right)_{r=0}=0 \text{ and } y_p(1,\tau)=y_b(\tau) \tag{57}$$

$$\frac{dy_b}{d\tau}=-2\frac{m_p/\rho_p}{V}\varepsilon_p\left(\frac{\partial y_p}{\partial r}\right)_{r=1} \text{ subject to } y_b(0)=0 \tag{58}$$

During derivation, infinitely long cylinders were considered, or end parts of the cylinders were assumed to be sealed regions to avoid mass transfer. To solve the above coupled differential equation, Laplace transform can be carried out to yield the following results.

$$sY_p(r,s)-1=\frac{1}{r}\frac{d}{dr}\left(r\frac{dY_p}{dr}\right)+\phi^2 Y_p$$

$$\text{subject to } \left(\frac{dY_p}{dr}\right)_{r=0}=0 \text{ and } Y_p(1,s)=Y_b(s) \tag{59}$$

$$sY_b(s)=-2\frac{m_p/\rho_p}{V}\varepsilon_p\left(\frac{\partial y_p}{\partial r}\right)_{r=1} \tag{60}$$

The above ordinary differential equations can be solved using Bessel function of the first kind with order zero and undetermined coefficient, A(s).

$$Y_b(r,s)=A(s)J_0(i\sqrt{s-\phi^2}\cdot r)+\frac{1}{s-\phi^2}$$

$$\text{and } Y_b(s)=2\frac{m_p/\rho_p}{V}\varepsilon_p\frac{A(s)}{s}i\sqrt{s-\phi^2}J_1(i\sqrt{s-\phi^2}) \tag{61}$$

Using the second boundary condition in Eq. (57), A(s) can be determined as the following equation from Eq. (61).

$$A(s)=\frac{s}{s-\phi^2}\frac{1}{2\frac{m_p/\rho_p}{V}\varepsilon_p i\sqrt{s-\phi^2}J_1(i\sqrt{s-\phi^2})-s\cdot J_0(i\sqrt{s-\phi^2})} \tag{62}$$

Thus, $Y_p(r, s)$ and $Y_b(s)$ can be solved in Laplace domain as the following results.

$$Y_p(r, s)=\frac{s}{s-\phi^2}\frac{J_0(i\sqrt{s-\phi^2}r)}{2\frac{m_p/\rho_p}{V}\varepsilon_p i\sqrt{s-\phi^2}J_1(i\sqrt{s-\phi^2})-s\cdot J_0(i\sqrt{s-\phi^2})}+\frac{1}{s-\phi^2}$$

and

$$Y_b(s)=\frac{1}{s-\phi^2}\frac{2\frac{m_p/\rho_p}{V}\varepsilon_p(i\sqrt{s-\phi^2})J_1(i\sqrt{s-\phi^2})}{2\frac{m_p/\rho_p}{V}\varepsilon_p i\sqrt{s-\phi^2}J_1(i\sqrt{s-\phi^2})-s\cdot J_0(i\sqrt{s-\phi^2})} \quad (63)$$

For inverse Laplace transform, poles should be found to apply residue theorem. Similar to spherical particles, the following operator, $\underline{\underline{L}}$ and eigenfunction, $\underline{K_n}$ can be defined to compute eigenvalues from eigenvalue equation, $\underline{\underline{L}}\underline{K_n}=-\xi_n^2\underline{K_n}$.

$$\underline{\underline{L}}=\begin{bmatrix}\frac{1}{r}\frac{d}{dr}\left(r\frac{d}{dr}\right)+\phi^2 & 0\\ -2\frac{m_p/\rho_p}{V}\varepsilon_p\left(\frac{d}{dr}\right)_{r=1} & 0\end{bmatrix} \text{ and } \underline{K_n}=\begin{bmatrix}K_n(r)\\ D_n\end{bmatrix} \quad (64)$$

Since the boundary conditions of eigenfunctions are $\left(\frac{dK_n(r)}{dr}\right)_{r=0}=0$ and $D_n=K_n(1)$, $K_n(r)$ and D_n can be solved as $K_n(r)=J_0(\lambda_n r)$ and $\sin\lambda_n$, respectively, when eigenvalue λ_n is defined as $\lambda_n^2=\xi_n^2+\phi^2$. For some values of ϕ and B, numerical values of λ_n are summarized in Table 4, which were calculated by solving the following nonlinear equation.

$$2\frac{m_p/\rho_p}{V}\varepsilon_p\lambda_n J_1(\lambda_n)+(\lambda_n^2-\phi^2)J_0(\lambda_n)=0 \quad (65)$$

For inverse Laplace transform, residues should be calculated in poles such as $s_n=i\sqrt{\phi^2-\lambda_n^2}$ or $s=\phi^2$, and the following solutions can be obtained by defining average concentration inside particles as $\bar{y}_p(\tau)=2\int_0^1 r y_p(r,\tau)dr$.

$$y_b(\tau)=\sum_{n=1}^{\infty}\frac{\left(\frac{\phi^2-\lambda_n^2}{\lambda_n^2}\right)\left(\frac{m_p/\rho_p}{V}\varepsilon_p\right)\exp\{(\phi^2-\lambda_n^2)\tau\}}{\left(\frac{m_p/\rho_p}{V}\varepsilon_p\right)^2+\left(\frac{m_p/\rho_p}{V}\varepsilon_p\right)+\frac{1}{4}\frac{(\phi^2-\lambda_n^2)^2}{\lambda_n^2}} \quad (66)$$

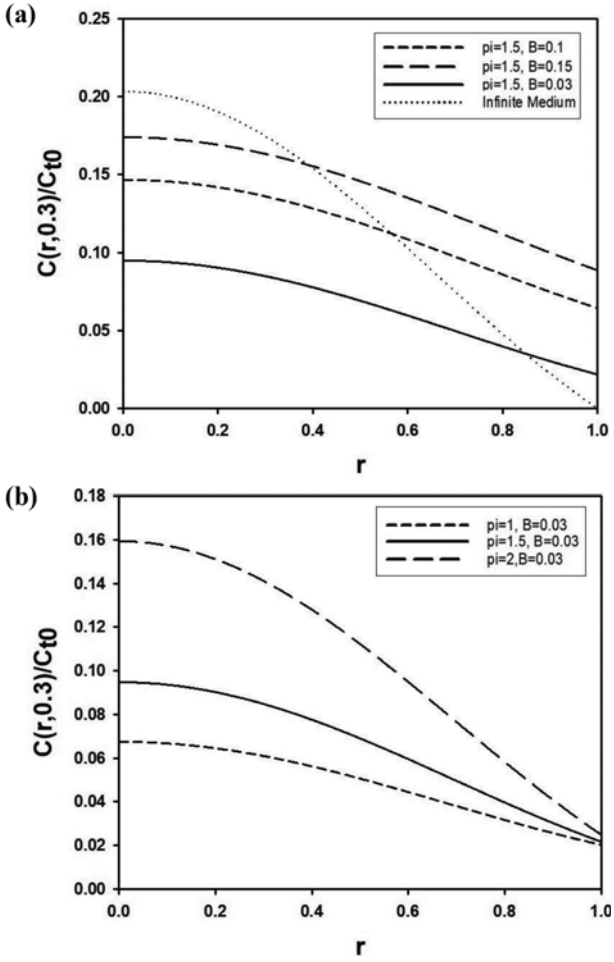

Fig. 11. Concentration profile of degradation product as a function of radial distance from the center of spherical PLGA particle immersed in liquid medium with volume, V, for (a) ϕ=1.5 and various values of B=$\frac{m_p/\rho_p}{V}\varepsilon_p$ and (b) B=0.03 and various values of ϕ. For all computation, dimensionless reaction time, τ, was assumed as 0.3.

$$y_p(r,\tau)=\sum_{n=1}^{\infty}\frac{\left(\frac{m_p/\rho_p}{V}\varepsilon_p\right)\left(\frac{\phi^2-\lambda_n^2}{\lambda_n^2}\right)^2 J_0(\lambda_n r)\exp\{(\phi^2-\lambda_n^2)\tau\}}{\left\{\left(\frac{m_p/\rho_p}{V}\varepsilon_p\right)^2+\left(\frac{m_p/\rho_p}{V}\varepsilon_p\right)+\frac{1}{4}\frac{(\phi^2-\lambda_n^2)^2}{\lambda_n^2}\right\}J_0(\lambda_n)} \quad (67)$$

Table 4. Eigenvalues λ_n of coupled differential equations of PLGA degradation system containing cylindrical PLGA particles for fixed value of B=$\frac{m_p/\rho_p}{V}\varepsilon_p$=0.03 and various values of ϕ

ϕ	λ_1	λ_2	λ_3	λ_4	λ_5	λ_6	λ_7	λ_8
0.1	0.099	2.429	5.531	8.661	11.797	14.935	18.074	21.214
0.5	0.492	2.43	5.531	8.661	11.797	14.935	18.074	21.214
1	0.983	2.434	5.531	8.661	11.797	14.935	18.074	21.214
1.5	1.469	2.444	5.532	8.661	11.797	14.935	18.074	21.214
1.75	1.707	2.454	5.532	8.661	11.797	14.935	18.074	21.214
2	1.935	2.474	5.533	8.661	11.797	14.935	18.074	21.214

$$\bar{y}_p(\tau)=\sum_{n=1}^{\infty}\frac{\left(\frac{\phi^2-\lambda_n^2}{\lambda_n^2}\right)^2\exp\{(\phi^2-\lambda_n^2)\tau\}}{\left(\frac{m_p/\rho_p}{V}\varepsilon_p\right)^2+\left(\frac{m_p/\rho_p}{V}\varepsilon_p\right)+\frac{1}{4}\frac{(\phi^2-\lambda_n^2)^2}{\lambda_n^2}} \quad (68)$$

Fig. 11 contains a concentration profile of degradation product as a function of dimensionless radial distance from the center of spherical PLGA particle. In Fig. 11(a), effect of volume fraction of the particle, B, on the concentration distribution was investigated for fixed value of dimensionless reaction time, τ, and Thiele modulus, ϕ, as 0.3 and 1.5, respectively. The calculation was performed by assuming initial concentration of the product in bulk medium as 0, and the results were compared with the profile inside spherical particle immersed in infinite medium (dotted line in Fig. 11(a)), as discussed in the previous section. Though all results were convex shape of the concentration distribution, concentration increased with increasing value of B, as shown in Fig. 11(a). The concentration at the particle surface (r=1) also increased with increasing value of B, indicating that higher bulk concentration can be obtained by increasing particle volume fraction in liquid medium, as discussed in Fig. 9(b). Since the results in Fig. 11(a) were computed after modeling degradation system with finite volume, they deviated from the results of spherical particles immersed in infinite medium (dotted line in Fig. 11(a)). When B was fixed as 0.03, the effect of Thiele modulus, ϕ, on the concentration distribution was also studied in Fig. 11(b). Though concentration increased drastically with increasing value of ϕ due to enhanced rate of decomposition reaction, the concentration at the particle surface increased slightly with increasing amount of spherical particles in liquid medium, when τ was fixed as 0.3.

Fig. 12(a) contains change of bulk concentration of degraded chemical species, $y_b(\tau)$, in finite liquid medium containing cylindrical PLGA particles, when B was fixed as 0.03. For ϕ=0.1 to 0.5, the concentration increased during early stage of the reaction and reached saturated value, implying that reaction rate was not so fast, causing insufficient feed rate of the degradation product generated from particles diffused to surrounding medium. However, drastic increase of the bulk concentration was observed with increasing value of ϕ. When ϕ and B were 2 and 0.03, respectively, increasing rate of bulk concentration was much faster than that of spherical particles, since surface to volume ratio of cylinder is smaller than sphere.

When B was fixed as 0.03, average concentration $\bar{y}_p(\tau)$ of the degradation product inside cylindrical particles suspended in finite medium was also plotted in Fig. 12(b) for various values of ϕ. When ϕ was small (ϕ=0.1 to 0.5), the average concentration inside cylindrical particles decreased rapidly during early stage and finally reached saturated value. However, the average concentration inside particles was recovered and increased consistently after short decreasing period during initial stage of degradation reaction, when ϕ was larger than 1. When ϕ and B were fixed as 2 and 0.03, respectively, $\bar{y}_p(\tau)$ and $y_b(\tau)$ were plotted together in Fig. 12(c). Since $\bar{y}_p(\tau)$ was always larger than $y_b(\tau)$ under fixed reaction conditions, outward flux from particle surface to bulk liquid was always guaranteed due to concentration difference, $\bar{y}_p(\tau)$-$y_b(\tau)$, as driving force.

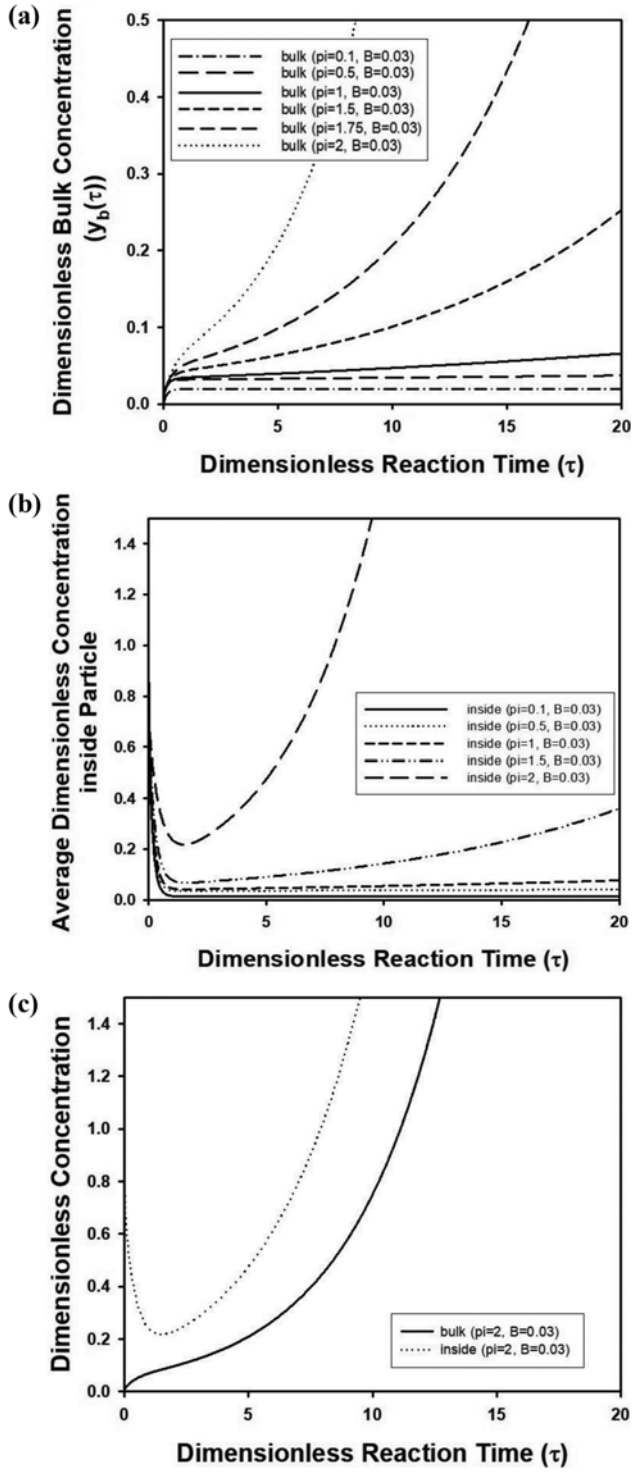

Fig. 12. Change of (a) bulk concentration of degradation product, $y_b(\tau)$ and (b) average dimensionless concentration of degradation product inside cylindrical particles, $\bar{y}_p(\tau)$, in liquid medium with finite volume, V, as a function of dimensionless reaction time for B=$\frac{m_p/\rho_p}{V}\varepsilon_p$=0.03 and various values of ϕ. (c) Change of $\bar{y}_p(\tau)$ inside cylindrical particles and $y_b(\tau)$ in surrounding medium with finite volume, V for ϕ=2 and B=0.03. Initial concentration of the degradation product in surrounding medium was assumed as 0.

In addition to spherical or cylindrical PLGA particles, slab-type particles suspended in liquid medium with finite volume were also studied for prediction of $\bar{y}_p(\tau)$ and $y_b(\tau)$ from the following coupled differential equation.

$$\frac{\partial y_p}{\partial \tau}=\frac{\partial^2 y_p}{\partial r^2}+\phi^2 y_p \text{ (for slab)}$$

$$\text{subject to } y_p(r,0)=1,\ \left(\frac{\partial y_p}{\partial r}\right)_{r=0}=0 \text{ and } y_p(1,\tau)=y_b(\tau) \tag{69}$$

$$\frac{dy_b}{d\tau}=-\frac{m_p/\rho_p}{V}\varepsilon_p\left(\frac{\partial y_p}{\partial r}\right)_{r=1} \text{ subject to } y_b(0)=0 \tag{70}$$

To solve the above equations, the following Laplace transform can be performed in Laplace domain instead of time domain.

$$sY_p(r,s)-1=\frac{d^2Y_p}{dr^2}+\phi^2 Y_p$$

$$\text{subject to } \left(\frac{dY_p}{dr}\right)_{r=0}=0 \text{ and } Y_p(1,s)=Y_b(s) \tag{71}$$

$$sY_b(s)=-\frac{m_p/\rho_p}{V}\varepsilon_p\left(\frac{\partial y_p}{\partial r}\right)_{r=1} \tag{72}$$

After solving the above ordinary differential equations, $Y_p(r,s)$ and $Y_b(s)$ can be found as the following results, which contains undetermined coefficient, A(s).

$$Y_p(r,s)=A(s)\cos(i\sqrt{s-\phi^2}\cdot r)+\frac{1}{s-\phi^2}$$

$$\text{and } Y_b(s)=\frac{m_p/\rho_p}{V}\varepsilon_p\frac{A(s)}{s}i\sqrt{s-\phi^2}\sin(i\sqrt{s-\phi^2}) \tag{73}$$

A(s) can be determined from the second boundary condition of Eq. (69) and Eq. (71) as the following result.

$$A(s)=\frac{s}{s-\phi^2}\frac{1}{\frac{m_p/\rho_p}{V}\varepsilon_p i\sqrt{s-\phi^2}\sin(i\sqrt{s-\phi^2})-s\cdot\cos(i\sqrt{s-\phi^2})} \tag{74}$$

Thus, the transient concentrations in Laplace domain can be derived as the following solutions.

$$Y_p(r,s)=\frac{s}{s-\phi^2}\frac{\cos(i\sqrt{s-\phi^2}r)}{\frac{m_p/\rho_p}{V}\varepsilon_p i\sqrt{s-\phi^2}\sin(i\sqrt{s-\phi^2})-s\cdot\cos(i\sqrt{s-\phi^2})}+\frac{1}{s-\phi^2}$$

and

$$Y_b(s)=\frac{1}{s-\phi^2}\frac{\frac{m_p/\rho_p}{V}\varepsilon_p(i\sqrt{s-\phi^2})\sin(i\sqrt{s-\phi^2})}{\frac{m_p/\rho_p}{V}\varepsilon_p i\sqrt{s-\phi^2}\sin(i\sqrt{s-\phi^2})-s\cdot\cos(i\sqrt{s-\phi^2})} \tag{75}$$

For inverse Laplace transform, the following differential operator and eigenfunction can be defined as matrix and vector form, respectively, to satisfy eigenvalue equation, $\underline{\underline{L}}\,\underline{K_n}=-\xi_n^2\underline{K_n}$.

$$\underline{\underline{L}}=\begin{bmatrix}\frac{d^2}{dr^2}+\phi^2 & 0\\ -\frac{m_p/\rho_p}{V}\varepsilon_p\left(\frac{d}{dr}\right)_{r=1} & 0\end{bmatrix} \text{ and } \underline{K_n}=\begin{bmatrix}K_n(r)\\ D_n\end{bmatrix} \tag{76}$$

When eigenvalue, λ_n, is defined as $\lambda_n^2=\xi_n^2+\phi^2$, eigenfunction $K_n(r)$ can be found as $K_n(r)=\cos(\lambda_n r)$ from $d^2K_n/dr^2=-\xi_n^2K_n$ and $\left(\frac{dK_n(r)}{dr}\right)_{r=0}=0$. D_n can be also determined as $D_n=\cos\lambda_n$ from boundary conditions such as $D_n=K_n(1)$. After substitution of these solutions to Eq. (76), the eigenvalues can be computed by solving the following nonlinear equation, and the numerical values of λ_n are summarized in Table 5 for selected values of ϕ and B.

$$\frac{m_p/\rho_p}{V}\varepsilon_p\lambda_n\sin\lambda_n+(\lambda_n^2-\phi^2)\cos\lambda_n=0 \tag{77}$$

Eigenvalues satisfying the above nonlinear equation can be computed by graphical or Newton-Raphson method, and the values are listed in Table 5 for specific values of $B=\frac{m_p/\rho_p}{V}\varepsilon_p$ and ϕ. Since

Table 5. Eigenvalues λ_n for various values of ϕ and $B=\frac{m_p/\rho_p}{V}\varepsilon_p$ coupled differential equations of PLGA degradation system containing slab-type PLGA particles

B	ϕ	λ_1	λ_2	λ_3	λ_4	λ_5	λ_6	λ_7
1.73×10^{-5}	2	1.571	2	4.712	7.854	10.996	14.137	17.279
	3	1.571	3	4.712	7.854	10.996	14.137	17.279
	6	1.571	4.812	6	7.854	10.996	14.137	17.279
	10	1.571	4.712	7.854	10	10.996	14.137	17.279
0.0003	2	1.568	2.003	4.713	7.854	10.996	14.137	17.279
0.03	2	1.542	2.031	4.72	7.858	10.998	14.139	17.281
0.3	2	1.377	2.211	4.788	7.895	11.024	14.159	17.296
3	0.01	0.005	2.456	5.233	8.205	11.256	14.343	17.449
	0.1	0.05	2.456	5.233	8.205	11.256	14.343	17.449
	0.5	0.248	2.473	5.237	8.206	11.257	14.344	17.449
	1	0.485	2.525	5.248	8.209	11.258	14.344	17.45
	2	0.883	2.739	5.296	8.224	11.264	14.347	17.451
30	2	0.352	3.082	6.104	9.142	12.19	15.245	18.307

poles of Eq. (75) can be $s_n=\phi^2-\lambda_n^2$ and $s=\phi^2$, $\bar{y}_p(\tau)$ and $y_b(\tau)$ can be found by inverse Laplace transform using residue theorem. In rectangular coordinates, average dimensionless concentration inside particles is defined as $\bar{y}_p(\tau)=\int_0^1 y_p(r,\tau)dr$.

$$y_b(\tau)=\sum_{n=1}^{\infty}\frac{2\left(\frac{m_p/\rho_p}{V}\varepsilon_p\right)\left(\frac{\phi^2-\lambda_n^2}{\lambda_n^2}\right)\exp\{(\phi^2-\lambda_n^2)\tau\}}{\left(\frac{m_p/\rho_p}{V}\varepsilon_p\right)^2+\left(\frac{m_p/\rho_p}{V}\varepsilon_p\right)\frac{\lambda_n^2+\phi^2}{\lambda_n^2}+\frac{(\phi^2-\lambda_n^2)^2}{\lambda_n^2}} \quad (78)$$

$$y_p(r,\tau)=\sum_{n=1}^{\infty}\frac{\frac{m_p/\rho_p}{V}\varepsilon_p\left(\frac{\phi^2-\lambda_n^2}{\lambda_n^2}\right)\cos(\lambda_n r)\exp\{(\phi^2-\lambda_n^2)\tau\}}{\left\{\left(\frac{m_p/\rho_p}{V}\varepsilon_p\right)^2+\left(\frac{m_p/\rho_p}{V}\varepsilon_p\right)\frac{\lambda_n^2+\phi^2}{\lambda_n^2}+\frac{(\phi^2-\lambda_n^2)^2}{\lambda_n^2}\right\}\cos(\lambda_n)} \quad (79)$$

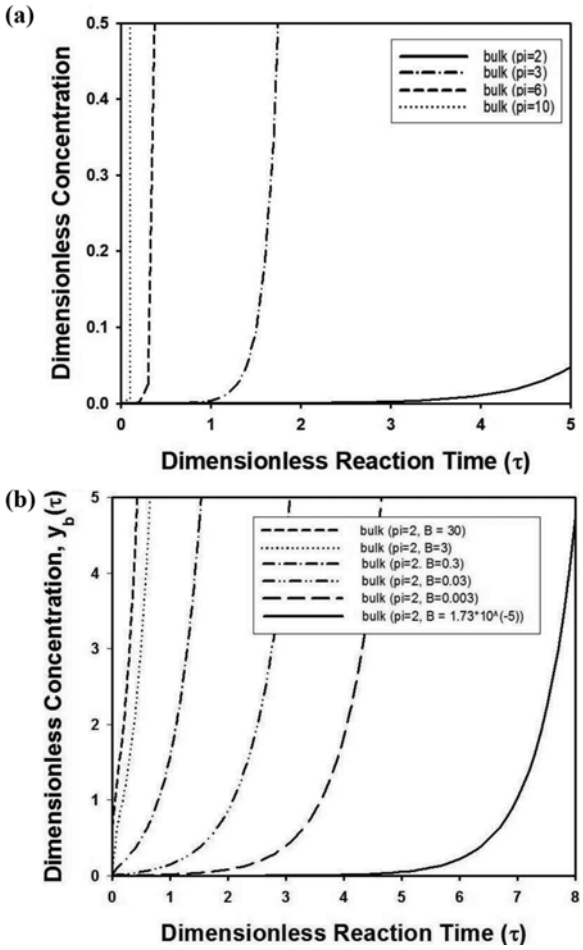

Fig. 13. Change of bulk concentration of degradation product, $y_b(\tau)$ in liquid medium with finite volume, V, containing slab-type PLGA particles as a function of dimensionless reaction time (a) for $B=\frac{m_p/\rho_p}{V}\varepsilon_p=1.73\times10^{-5}$ and various values of ϕ and (b) for $\phi=2$ and various values of B. Initial concentration of the degradation product in surrounding medium was assumed as 0.

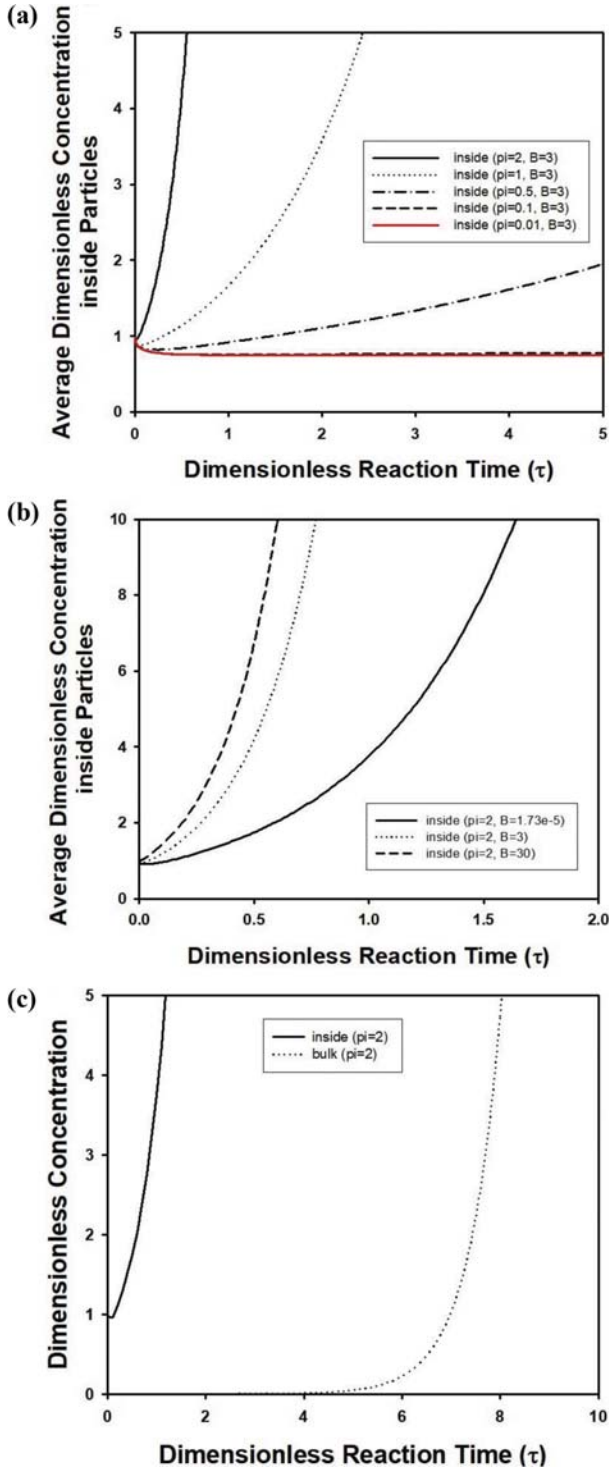

Fig. 14. Change of average dimensionless concentration of degradation product inside slab-type particles, $\bar{y}_p(\tau)$ in liquid medium with finite volume, *V*, as a function of dimensionless reaction time (a) for $B=\frac{m_p/\rho_p}{V}\varepsilon_p=3$ and various values of ϕ and (b) for $\phi=2$ and various values of B. (c) Change of $\bar{y}_p(\tau)$ inside cylindrical particles and $y_b(\tau)$ in surrounding medium with finite volume, V for $\phi=2$ and $B=1.73\times10^{-5}$. Initial concentration of the degradation product in surrounding medium was assumed as 0.

$$\bar{y}_p(\tau)=\sum_{n=1}^{\infty}\frac{2\left(\frac{\phi^2-\lambda_n^2}{\lambda_n^2}\right)^2\exp\{(\phi^2-\lambda_n^2)\tau\}}{\left(\frac{m_p/\rho_p}{V}\varepsilon_p\right)^2+\left(\frac{m_p/\rho_p}{V}\varepsilon_p\right)\frac{\lambda_n^2+\phi^2}{\lambda_n^2}+\frac{(\phi^2-\lambda_n^2)^2}{\lambda_n^2}} \quad (80)$$

Fig. 13(a) contains change of bulk concentration in finite medium containing very dilute amount of slab-type PLGA particle (B=1.73×10^{-5}) for various values of ϕ. When ϕ was larger than 3, very steep increase of the concentration of degraded component was observed, whereas very low bulk concentration was maintained for $0<\tau<3$, when ϕ was 2. The effect of the amount of slab-type PLGA particles was also studied, and the results are displayed in Fig. 13(b). When the suspension of slab-type particles became more concentrated, the increasing rate of bulk concentration of degraded components became faster, since molar flow rate of the reaction product from the particles increased.

In Fig. 14(a), the average concentration inside slab-type particles was also computed for various values of ϕ, when B was fixed as 3, which is a very concentrated condition. For all cases, slight decrease of the average concentration was observed in initial stage of reaction. When ϕ was smaller than 0.1, the decrease continued with reaction time, whereas concentration increased after initial period for larger value of ϕ (>0.5). For very small values of Thiele modulus such as ϕ=0.01 and 0.1, there was negligible difference between transient behavior of the concentration inside slab-type particles. For ϕ=2, average concentration of the degraded product inside slab-type particles was also plotted in Fig. 14(b), which shows consistent increase of the concentration of degraded component with reaction time due to sufficiently large value of Thiele modulus. The increasing rate became faster for more concentrated suspension with large value of B such as 3 or 30. Similar to spherical or cylindrical PLGA particles, concentration in bulk liquid, $\bar{y}_p(\tau)$ and average concentration inside slab-type particles, $y_b(\tau)$, were also compared in Fig. 14(c) for ϕ=2 and B=1.73×10^{-5}. Since the concentration difference of $\bar{y}_p(\tau)$ and $y_b(\tau)$ was always positive, flowing direction of degraded component from particle to bulk medium was confirmed during the reaction.

4. Calculation of Mass Flux from Particle Surface to Bulk Medium with Finite Volume

In this study, the following molar flux from particle surface was calculated by applying Fick's first law in Eqs. (56), (67), and (79) for spherical, cylindrical, and slab-type particles, respectively. For convenience, the initial concentration distribution inside the particles was assumed as uniform profile, whereas concentration in bulk surrounding medium was considered as zero.

(For sphere)

$$-D\frac{C_{t0}}{R}\left(\frac{\partial y_p}{\partial r}\right)_{r=1}=$$

$$6D\frac{C_{t0}}{R}\sum_{n=1}^{\infty}\frac{\frac{(\phi^2-\lambda_n^2)^2}{\lambda_n^2}\exp\{(\phi^2-\lambda_n^2)\tau\}}{3\left(\frac{m_p/\rho_p}{V}\varepsilon_p\right)^2+\left(3\frac{m_p/\rho_p}{V}\varepsilon_p\right)\frac{2\lambda_n^2-\phi^2}{\lambda_n^2}+\frac{(\phi^2-\lambda_n^2)^2}{\lambda_n^2}} \quad (81)$$

(For cylinder)

$$-D\frac{C_{t0}}{R}\left(\frac{\partial y_p}{\partial r}\right)_{r=1}=$$

$$2D\frac{C_{t0}}{R}\sum_{n=1}^{\infty}\frac{\frac{(\phi^2-\lambda_n^2)^2}{4\lambda_n^2}\exp\{(\phi^2-\lambda_n^2)\tau\}}{\left(\frac{m_p/\rho_p}{V}\varepsilon_p\right)^2+\left(\frac{m_p/\rho_p}{V}\varepsilon_p\right)+\frac{(\phi^2-\lambda_n^2)^2}{4\lambda_n^2}} \quad (82)$$

(For slab)

$$-D\frac{C_{t0}}{R}\left(\frac{\partial y_p}{\partial r}\right)_{r=1}=$$

$$2D\frac{C_{t0}}{R}\sum_{n=1}^{\infty}\frac{\frac{(\phi^2-\lambda_n^2)^2}{\lambda_n^2}\exp\{(\phi^2-\lambda_n^2)\tau\}}{\left(\frac{m_p/\rho_p}{V}\varepsilon_p\right)^2+\left(\frac{m_p/\rho_p}{V}\varepsilon_p\right)\frac{\lambda_n^2-\phi^2}{\lambda_n^2}+\frac{(\phi^2-\lambda_n^2)^2}{\lambda_n^2}} \quad (83)$$

The eigenvalues, λ_n, in the above Eqs. (81), (82), and (83) satisfy Eqs. (53), (65), and (77), respectively. Fig. 15 contains molar flux of degraded component as a function of dimensionless reaction time, when Thiele modulus ϕ and particle volume fraction, B were fixed as 2 and 0.03, respectively. Except a very short starting period, the magnitude of the flux from the particle surface was in the order of sphere<cylinder<slab. Since ϕ was sufficiently large, molar flux increased with increasing reaction time, implying that generation of the degraded component resulted in material transport toward bulk liquid.

The models describing decomposition of polymer particles can be applied for prediction of biodegradation of polymeric materials in medical engineering. In dental application, biodegradable films can be adopted for various surgeries, whereas biological scaffolds with woodpile structure consisting of biodegradable polymers can

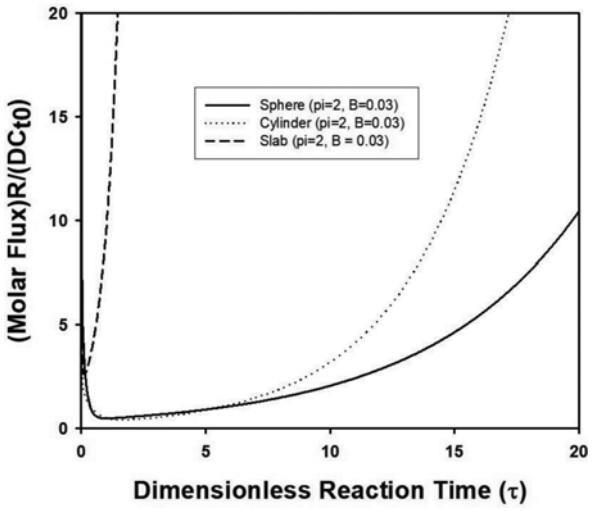

Fig. 15. Molar flux of degraded product from the surface of spherical, cylindrical, and slab-type particle surrounded in liquid medium with finite volume, V as a function of dimensionless reaction time, τ. B and ϕ were fixed as 0.03 and 2, respectively.

be used for cell culture by combining 3D printing technology [23, 24]. Electrospinning can be also applied to prepare infinitely long cylinders of polylactic acid for tissue engineering [25]. Recently, spherical particles of biodegradable polymers have attracted much attention as drug carrier [26]. In these medical applications, our model can be used for accurate prediction of concentration of degraded components in living systems. In addition to concentration inside particles with various morphologies, bulk concentration outside the particles can be also predicted from our model, which is useful for estimation of dissolution phenomena of degraded component into human body or culture medium.

CONCLUSIONS

The degradation of PLGA particles with various morphologies such as spherical, cylindrical, or slab-type particles was modeled to predict concentration of degraded product, assuming that degradation reaction follows the first-order kinetics. As the first approach, a PLGA particle suspended in infinite medium was considered to compute the concentration of the degradation product inside the particle. To solve reaction-diffusion equations, eigenfunction expansion method was applied for prediction of the concentration as a function of reaction time and radial distance from the center of the particles. Concentration at the central position as well as average concentration was predicted for three types of particles with the rate constant of the first-order reaction as variable parameter. With increasing Thiele modulus, average concentration inside particle increased as a function of reaction time after short decreasing period in early stage of the degradation reaction. Among three kinds of the particles, the highest concentration was observed from slab-type particle under the same reaction condition due to smallest surface to volume ratio of the particle, causing least amount of mass flow rate of the degraded component to bulk medium.

To modify calculation results obtained by assuming infinite *Biot* number, diffusional resistance inside particles to convective resistance in bulk medium was also considered for isolated particles immersed in infinite medium using *Biot* number as variable parameter. The reaction diffusion equations for three types of particles were also solved by eigenfunction expansion method to solve the concentration as a function of time, radial distance, as well as *Biot* number. With decreasing *Biot* number, the concentration of degradation product inside particles increased drastically due to increase of mass transfer resistance in surrounding fluid.

To reflect real degradation system with finite amount of liquid medium, modeling was carried out to predict bulk concentration as well as the concentration inside particles with various morphologies. Coupled differential equations were solved by Laplace transform, applying residue theorem for inversion. For all cases, bulk concentration was always smaller than average concentration of degraded product inside particles, implying that the direction of mass flow was always from the particle surface toward liquid medium. In addition to Thiele modulus, the volume fraction of the particles suspended in the medium also affected the concentration. Higher bulk concentration was predicted from more concentrated suspension due to larger flux of degraded component from particle surface to surrounding medium. Among three types of the particle morphologies, smallest concentration in bulk phase and inside particles was observed under the same reaction conditions, whereas slab-type particles showed the highest concentration.

ACKNOWLEDGEMENTS

This research was supported by Priority Research Centers Program through the National Research Foundation of Korea (NRF) funded by the Ministry of Education (NRF-2017R1A6A1A03015562) and Korea Institute for Advancement of Technology (KIAT) grant funded by the Korea Government (MOITIE, P0002007, The Competency Development Program for Industry Specialist).

REFERENCES

1. N. Iqbal, A. S. Khan, A. Asif, M. Yar, J. W. Haycock and I. U. Rehman, *Int. Mater. Rev.*, **64**(2), 91 (2018).
2. G. Rebagay and S. Bangalore, *Curr. Cardiovasc. Risk Rep.*, **13**(22), 2 (2019).
3. P. Kallinteri, S. Higgins, G. A. Hutcheon, C. B. St. Pourcain and M. C. Garnett, *Biomacromolecules*, **6**, 1885 (2005).
4. J. M. Anderson and M. S. Shive, *Adv. Drug Deliv. Rev.*, **28**, 5 (1997).
5. C. E. Astete and C. M. Sabliov, *J. Biomater. Sci. Polym. Ed.*, **17**(3), 247 (2006).
6. M. S. Lopes, A. L. Jardini and R. M. Filho, *Chem. Eng. Trans.*, **38**, 331 (2014).
7. E. Swider, O. Koshkina, J. Tel, L. J. Cruz, I. Jolanda M. de Vries and M. Srinivas, *Acta Biomater.*, **73**, 38 (2018).
8. F. Danhier, E. Ansorena, J. M. Silva, R. Coco, A. Le Breton and V. Préat, *J. Controlled Release*, **161**(2), 505 (2012).
9. C.-C. Yu, Y.-W. Chen, P.-Y. Yeh, Y.-S. Hsiao, W.-Ti. Lin, C.-W. Kuo, D.-Y. Chueh, Y.-W. You, J.-J. Shyue, Y.-C. Chang and P. Chen, *J. Nanobiotechnol.*, **17**(1), 31 (2019).
10. X. Liu, S. G. Baldursdottir, J. Aho, H. Qu, L. P. Christensen, J. Rantanen and M. Yang, *Pharm. Res.*, **34**, 738 (2017).
11. C. F. van Nostrum, T. F. J. Veldhuis, G. W. Bos and W. E. Hennink, *Polymer*, **45**, 6779 (2004).
12. P. Blasi, *J. Pharm. Investig.*, **49**, 337 (2019).
13. A. N. F. Versypt, P. D. Arendt, D. W. Pack and R. D. Braatz, *Plos One*, **10**(8), e0135506 (2015).
14. E. Vey, C. Rodger, J. Booth, M. Claybourn, A. F. Miller and A. Saiani, *Polym. Degrad. Stab.*, **96**, 1882e1889 (2011).
15. D. H. Kim and J. Lee, *Korean J. Chem. Eng.*, **29**(1), 42 (2012).
16. N. Bessonov, G. Bocharov, A. Meyerhans, V. Popov and V. Volpert, *Mathematics*, **8**, 117 (2020).
17. Y.-S. Cho, *Korean Chem. Eng. Res.*, **57**(5), 652 (2019).
18. W. Cho and J. Lee, *Korean J. Chem. Eng.*, **30**(3), 580 (2013).
19. A. K. Mohammad and J. J. Reineke, *Mol. Pharm.*, **10**(6), 2183 (2013).
20. K. K. Chereddy, V. L. Payen and V. Préat, *J. Controlled Release*, **289**, 10 (2018).
21. R. G. Rice and D. D. Do, *Applied mathematics and modeling for chemical engineers*, 1st Ed., John Wiley & Sons, New York (1995).
22. B. Amoyav and O. Benny, *Polymers*, **11**, 419 (2019).
23. Z. B. Ahi, N. Z. Renkler, M. G. Seker and K. Tuzlakoglu, *Int. J. Biomater.*, **2019**, 1932470 (2019).
24. G. D. Giustina, A. Gandin, L. Brigo, T. Panciera, S. Giulitti, P. Sgar-

bossa, D. D'Alessandro, L. Trombi, S. Danti and G. Brusatin, *Mater. Des.*, **165**, 107566 (2019).
25. J. Lannutti, D. Reneker, T. Ma, D. Tomasko and D. Farson, *Mater. Sci. Eng. C*, **27**(3), 504 (2007).
26. T. Ryu, S. E. Kim, J.-H. Kim, S.-K. Moon and S.-W. Choi, *J. Bioact. Compat. Polym.*, **29**(5), 445 (2014).